AD-A152 197 RESEARCH AND DEVELOPMENT OF SUBSURFACE ACOUSTIC WAVE DEVICES FOR SENSOR A..(U) UNITED TECHNOLOGIES RESEARCH CENTER EAST HARTFORD CT D E CULLEN ET AL. JAN 85 1/1

UNCLASSIFIED UTRC/R85-926671 AFOSR-TR-85-0260 F/G 20/1 NL

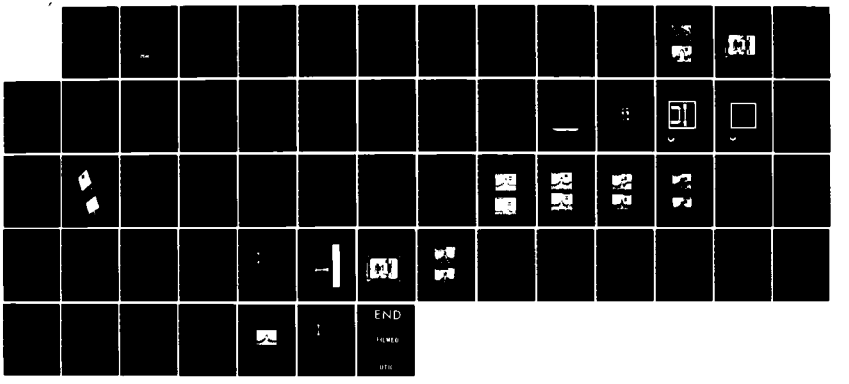

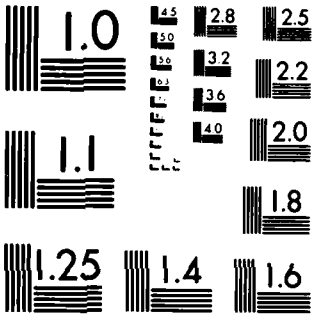

MICROCOPY RESOLUTION TEST CHART
NATIONAL BUREAU OF STANDARDS-1963-A

RESEARCH AND DEVELOPMENT OF SUBSURFACE ACOUSTIC WAVE DEVICES FOR SENSOR APPLICATIONS

D.E. Cullen
T.W. Grudkowski

Report No. 85-926671

Final Report Period Covered:
November 30, 1983—January 31, 1985

Air Force Office of Scientific Research
Bolling AFB, D.C. 20332
Contract No. F49620-84-C-0006

UNITED TECHNOLOGIES RESEARCH CENTER

UNCLASSIFIED

SECURITY CLASSIFICATION OF THIS PAGE (When Data Entered)

REPORT DOCUMENTATION PAGE

READ INSTRUCTIONS BEFORE COMPLETING FORM

1. REPORT NUMBER: AFOSR-TR- 85-0260	2. GOVT ACCESSION NO.: AD-A152197
3. RECIPIENT'S CATALOG NUMBER:	
4. TITLE (and Subtitle): Research & Development of Subsurface Acoustic Wave Devices for Sensor Applications	5. TYPE OF REPORT & PERIOD COVERED: Final Technical Report Nov. 30, 1983 - Jan. 31, 1985
	6. PERFORMING ORG. REPORT NUMBER: R85-926671
7. AUTHOR(s): Donald E. Cullen, Thomas W. Grudkowski	8. CONTRACT OR GRANT NUMBER(s): F49620-84-C-0006
9. PERFORMING ORGANIZATION NAME AND ADDRESS: United Technologies Research Center, East Hartford, CT 06108	10. PROGRAM ELEMENT, PROJECT, TASK AREA & WORK UNIT NUMBERS: 61102F, 2305, B2
11. CONTROLLING OFFICE NAME AND ADDRESS: Air Force Office of Scientific Research, Bldg. 410, Bolling Air Force Base, D.C. 20332	12. REPORT DATE: January, 1985
	13. NUMBER OF PAGES: 67
14. MONITORING AGENCY NAME & ADDRESS (if different from Controlling Office)	15. SECURITY CLASS. (of this report): Unclassified
	15a. DECLASSIFICATION/DOWNGRADING SCHEDULE

16. DISTRIBUTION STATEMENT (of this Report)

Approved for public release; distribution unlimited.

17. DISTRIBUTION STATEMENT (of the abstract entered in Block 20, if different from Report)

18. SUPPLEMENTARY NOTES

19. KEY WORDS (Continue on reverse side if necessary and identify by block number)

Surface Skimming Bulk Waves (SSBW), SSBW Sensors, SSBW Strain Sensitivity,

20. ABSTRACT (Continue on reverse side if necessary and identify by block number)

Surface skimming bulk waves (SSBW) in quartz were examined for sensor applications. Sensitivities to substrate strains, temperature, and fluid immersion were determined for AT and BT-cut quartz. The application of a strain sensitive SSBW device configuration as a fluid damped, cantilever beam accelerometer was investigated.

This program has resulted in the discovery of an SSAW mode with properties that are extremely well suited to the development of acoustic wave sensors.

DD FORM 1 JAN 73 1473 EDITION OF 1 NOV 65 IS OBSOLETE

S/N 0102-LF-014-6601

UNCLASSIFIED

SECURITY CLASSIFICATION OF THIS PAGE (When Data Entered)

ORIGINATOR - SUPPLIED KEY WORDS INCLUDE:

R85-926671

Research and Development of Subsurface Acoustic Wave Devices for Sensor Applications

TABLE OF CONTENTS

ABSTRACT

Surface skiming bulk waves (SSBW) in quartz were examined for sensor applications. Sensitivities to substrate strains, temperature, and fluid immersion were determined experimentally for AT and BT-cut quartz. The application of a strain sensitive SSBW device configuration as a fluid damped, cantilever beam accelerometer was investigated.

This program has resulted in the discovery of an SSAW mode with properties that are extremely well suited to the development of acoustic wave sensor. The SSBW in BT-cut quartz has: (1) a higher strain sensitivity than any other known SSAW mode (approximately 2 ppm/microstrain), (2) a very low temperature sensitivity (zero first order temperature coefficient and 0.03 ppm/$^{\circ}C^2$ second order coefficient), and (3) a relatively low sensitivity to surface fluids (< 6 dB attenuation). The potential for practical sensors based upon the strain sensitivity of the SSBW mode in BT-cut quartz is believed to be excellent.

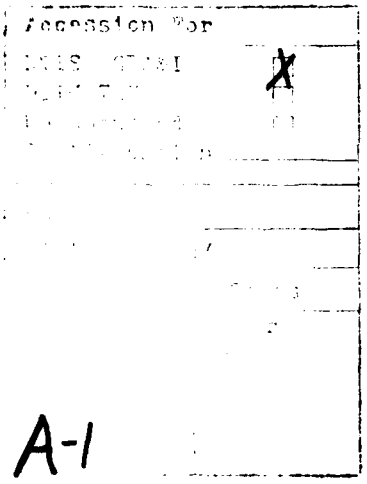

ACKNOWLEDGEMENTS

The authors are pleased to acknowledge the individuals who made important contributions during the course of this program. Dr. A. J. DeMaria and G. K. Montress provided program management with helpful suggestions and guidance to the technical effort. R. Basilica fabricated all of the experimental devices. S. Sheades assisted in the measurement of device characteristics.

Research and Development of Subsurface Acoustic Wave Devices for Sensor Applications

1.0 INTROUCTION

1.1 Program Scope and Objectives

This research and development program conducted by the United Technologies Research Center was directed toward a more complete understanding of subsurface acoustic wave (SSAW) modes and the continued development of SSAW devices for sensor applications. The program was a logical continuation of the fundamental theoretical and experimental investigation of SSAW configurations performed under the predecessor AFOSR Contract No. F49620-82-C-0074 (Ref. 1). The principal objectives of the present program were: (1) to experimentally measure the sensor related properties of the most promising SSAW configuration, (2) to optimize that configuration for sensor applications, and (3) to build and evaluate a laboratory prototype SSAW accelerometer. The primary goal of the program was to show that practical acoustic wave sensors could be realized by demonstrating the performance characteristics of a laboratory SSAW accelerometer and then using those results to predict the performance of a more fully developed accelerometer.

1.2 Background and Method of Approach

Surface-oriented acoustic waves which propagate on or within close proximity of the surface of a piezoelectric medium are finding extensive applications as delay lines, filters, oscillator frequency control elements, and as signal processing elements. The major attractive feature of these waves is the ability to electrically excite, detect, and otherwise influence their propagation characteristics and frequency response through the use of metallic electrode patterns which are distributed on or near the substrate surface. The resulting small size, light weight, and design precision of these devices have led to their preferred use in numerous system applications. These waves are also capable of sensing external perturbations to the propagation media through the effect of stress or surface ambient conditions on the acoustic wave velocity. This latter property may be either minimized or maximized for a particular application depending on the choice of substrate material and propagation mode.

For the present accelerometer sensor application, the choice is directed toward maximizing sensitivity to bending strain, while minimizing sensitivity

to surface ambient conditions such as temperature, surface contaminants, and surface loading caused by intentional submersion within a vibration damping fluid. The preservation of the superior frequency stability and frequency response characteristics, typical of acoustic wave device technology, is also required.

Two major classes of surface-oriented acoustic waves, Surface Acoustic Waves (SAW) and SSAW, have examined for sensor applications. SAW sensors suffer from extreme sensitivity to surface contaminants and SAW's are completely attenuated by any fluid in contact with the propagation surface. Efforts to encapsulate SAW devices within sealed packages also lead to unstable package-induced strains which are unpredictable and degrade sensor accuracy and sensitivity. In contrast, SSAW sensors utilizing acoustic waves which propagate beneath but within a few wavelengths of the surface have been shown to have low sensitivity to surface contaminants and surface fluids (Ref. 1) so that the severe packaging problems are avoided. In addition, SSAW modes may be found which have the desired high strain sensitivity and low temperature sensitivity necessary for sensor applications while preserving the required stability and performance characteristics of SAW's.

During the previous contract (Ref. 1), several SSAW substrate configurations and modes were theoretically and experimentally investigated. The major configurations involved: 1) a layered media structure in which a thin dielectric, non-piezoelectric film was vacuum deposited onto a piezoelectric substrate, and 2) a single crystal piezoelectric substrate for which SSAW modes can exist for certain crystal orientations. Several material combinations were investigated for the layered structure, resulting in the discovery of new modes of SSAW propagation having both low sensitivity to surface loading and low temperature sensitivity. In particular, the generalized Stoneley wave mode in a SiO_2 coated, 128° rotated Y-cut lithium niobate substrate was found to have moderate strain sensitivity, a zero first order temperature coefficient, and propagation characteristics suitable for sensor applications. For the single crystal configuration, the Surface Skimming Bulk Wave (SSBW) on AT-cut quartz was found to possess similar potential for sensor development. Strain sensitivities for these configurations were the first to be reported in the literature (Ref. 4, 5).

A technical decision concerning the selection of the single crystal quartz configurations was made early within the present program for the following reasons. First, reproducibility of the layered substrate results was strongly dependent on the thin film deposition parameters, probably caused by stresses in the film. This nonreproducibility could be elliminated through a thorough parametric investigation of deposition techniques and annealing processes. However, residual interfacial stresses or induced stress upon exercising of the sensor may still lead to instabilities that would limit the usefullness of the sensor. Second, the initial results achieved for the quartz configuration resulted in greater strain sensitivity and extremely good reproducibility. Discussions with

the Contract monitor indicated that further focus on the several potential SSAW modes on quartz would have the greatest probability for program success and was therefore adopted as the approach for development under this program. The prgram was devoted to a study of SSBW modes in quartz: their strain sensitivity, temperature sensitivity, sensitivity to surface fluids to an optimization of the SSBW delay line design for sensor use; and to the design fabrication, testing, and evaluation of a laboratory prototype SSBW accelerometer.

1.3 Description of Program Tasks

This program was divided into three distinct tasks. In Task I, two candidate SSAW configurations were to be considered for selection as the primary structure to be developed within Tasks II and III. These candidates included the surface skimming bulk wave (SSBW) in -36° rotated Y-cut quartz and the generalized Stoneley wave (GSW) in SiO_2 coated, 128° rotated Y-cut lithium niobate. Of the several configurations previously investigated (Ref. 1), these two showed the most promise for practical device realization. This Task resulted in the selection of the SSBW quartz configuration based on its superior potential for high accuracy, reproducible sensor development.

Task II involved the optimization of the selected SSAW structure. The effort was directed toward achieving a practical SSAW delay line having optimized strain sensitivity, minimum temperature coefficient of time delay, and spurious free bandpass frequency response. Fabrication methods were optimized as required to reproducibly achieve the desired SSAW propagation characteristics. The design of the launching and receiving SSAW interdigital transducers were optimized through electrical equivalent circuit analysis and experimental diagnostic measurements. Diagnostic transducer structures were fabricated and examined to provide data on the magnitude of the acoustoelectric coupling of the SSAW mode, acoustic propagation loss, and frequency dependence as a basis for design optimization. The frequency response of the resulting two-port SSAW delay line, consisting of input and output interdigital transducers was optimized for minimum insertion loss (IL) (<32 dB achieved), low spurious content (<0.01 dB bandpass ripple), and bandpass shape (Q = 550 to 750) suitable for use in an electronic oscillator circuit. Experimental delay lines were designed for operation over the 120 to 640 MHz frequency range. The strain sensitivity of delay lines operating at several frequencies within this range was measured in order to determine the dependence upon operating frequency. The frequency dependence was found to be negligible. Figure 1-1 shows the frequency response of a typical SSBW device on quartz illustrating the very low spurious content, the linear phase characteristic, and the effect of fluid loading.

A laboratory prototype acceleration sensor was designed, fabricated, tested, and evaluated in Task III. The SSAW delay line was designed for an optimized

bandpass frequency response as determined by Task II results. The acoustic delay line was then fabricated on a cantilever beam at at the proper position so as to achieve maximum strain sensitivity. An electronic oscillator circuit was designed and implemented using the quartz SSAW delay line as the frequency determining element. The frequency shift of the resulting oscillator due to a 2G change in acceleration was measured and compared with predicted sensitivity. The performance characteristics of this laboratory accelerometer were then used to predict the level of performance of a more fully developed SSAW accelerometer. A photo of one of the experimental SSBW accelerometers is shown in Fig. 1-2.

1.4 Summary of the Report

Section 2 details the investigation of the sensor related properties of both AT and BT-cut quartz SSBW devices. The design and evaluation of the laboratory prototype accelerometer based upon SSBW's in BT-cut quartz is described in Section 3. Section 4 presents a brief summary of the program and gives the recommendations for continued development of the SSBW sensor technology.

This program has resulted in the discovery of an SSAW mode with properties that are extremely well suited to the development of acoustic wave sensors. The SSBW in BT-cut quartz has: (1) a higher strain sensitivity than any other known SSAW mode (approximately 2 ppm/microstrain), (2) a very low temperature sensitivity (zero first order temperature coefficient and 0.03 ppm/°C second order coefficient), and (3) a relatively low sensitivity to surface fluids (<6 dB attenuation). The potential for practical sensors based upon the strain sensitivity of the SSBW mode in BT-cut quartz is believed to be excellent.

During the period of this program, a paper entitled "Strain Sensitivity of SSBW's in Quartz" was presented at the 1984 IEEE Ultrasonics Symposium in Dallas, and the text of the paper will be published in the proceedings of that symposium. A preprint of the text is included as Appendix A.

FIG. 1-1

IL CHARACTERISTICS OF SSBW ON BT-CUT QUARTZ

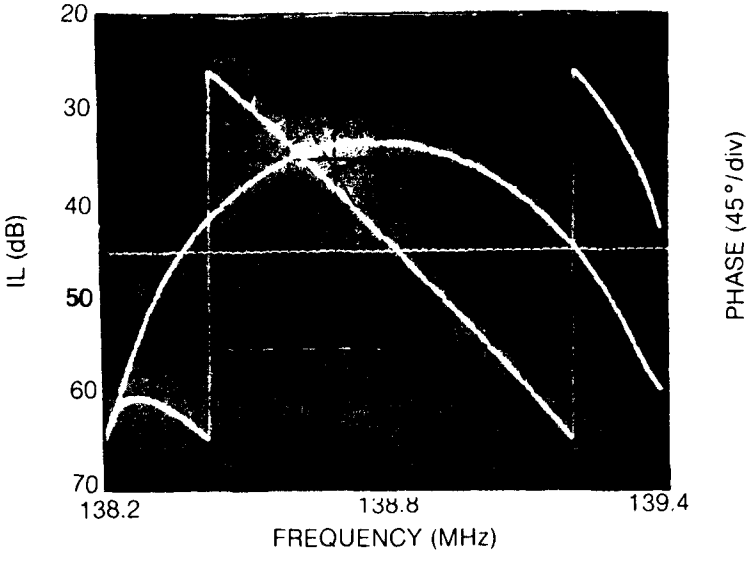

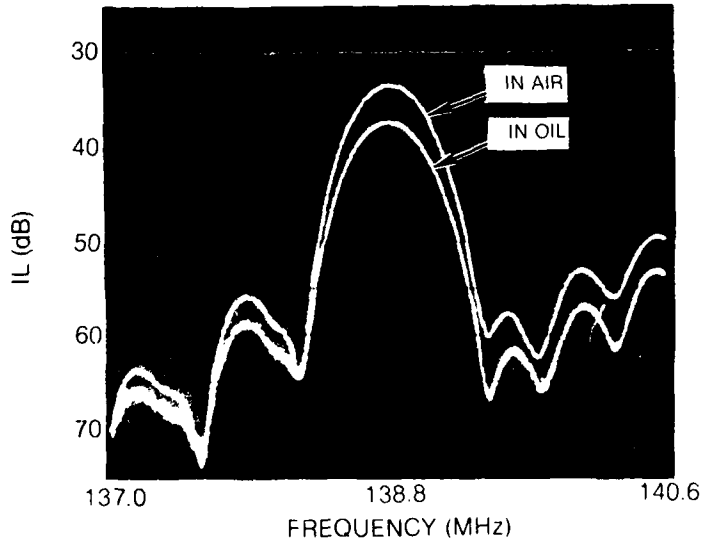

85-1-28-12

LABORATORY SSBW ACCELEROMETER

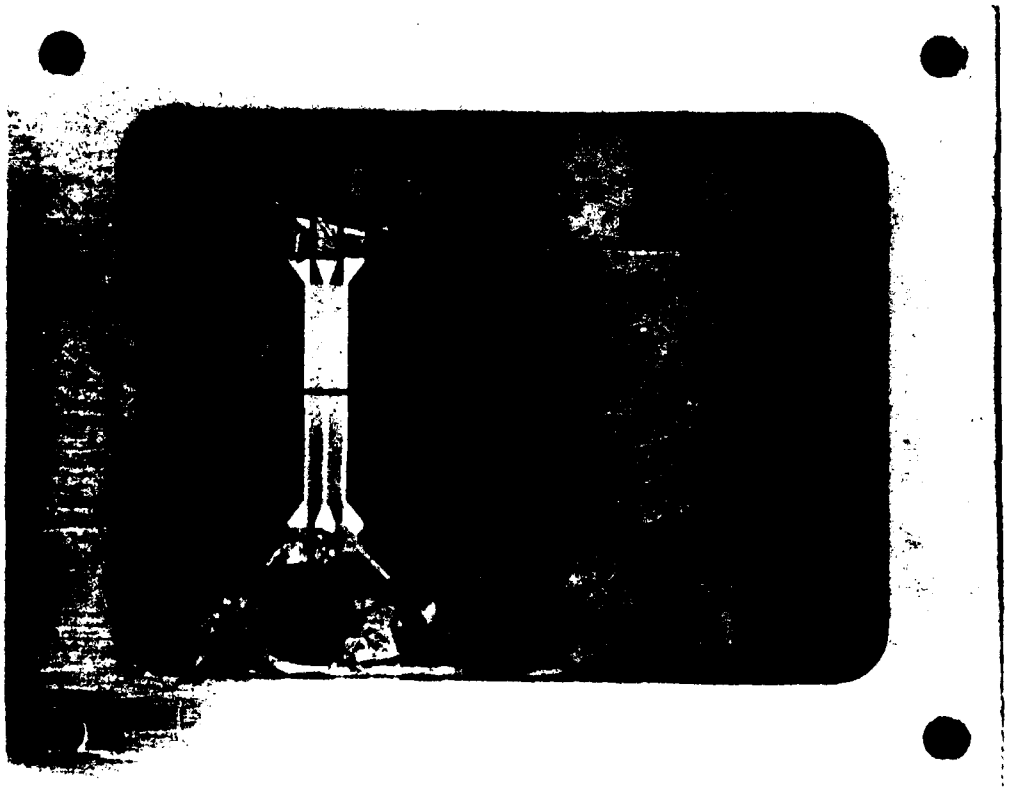

2.0 SSBW DEVICE DEVELOPMENT

2.1 Introduction

The principal characteristics of SSBW propagation that are essential to the development of SSBW sensors have been studied for the two temperature compensated cuts of quartz. Work with SSBW's in -36° rotated Y-cut quartz (AT-cut quartz) was initiated during the prior Contract (Ref. 1) and continued during this program. Since it is known (Refs. 2 and 3) that there is another singly rotated Y-cut of quartz with a zero first order temperature coefficient for SSBW's (+50.5° rotated Y-cut or BT-cut), devices were fabricated on BT-cut quartz substrates and their sensor related properties examined experimetally. The SSBW delay line design was optimized to provide minimum insertion loss and spurious free bandpass characteristics. Table 2-1 is a summary of the devices examined during the course of this program showing the type of measurements made on each device.

2.2 SSBW Delay Line Design Considerations

Figure 2-1 shows plan and cross-sectional views of a SSBW device. The cross-sectional view indicates the crystallographic orientation of a BT-cut substrate and shows schematically the far-field radiation pattern of the SSBW. The operation of a SSBW delay line is readily understood in terms of antenna theory, with the interdigital transducers acting as endfire array antennas. Only at the synchronous frequency (or at odd harmonics of the synchronous frequency), determined by the shear wave velocity and the periodicity of the interdigital transducer, is energy radiated along the surface as shown in the figure. At other frequencies the energy is radiated into the bulk of the crystal.

The plan view in Fig. 2-1 illustrates the basic delay line configuration with the simplest two-finger-per-wavelength (λ) interdigital transducer pattern. This transducer pattern, with $\lambda/4$ fingers and gaps, is not often used in practice because of the large spurious signals generated by this type of design. More often, a "double-electrode" or "split-finger" transducer with $\lambda/8$ fingers and gaps is employed. In this design, reflected signals from adjacent electrodes are 180° out of phase with one an other, hence the total reflected signal is minimized. All of the SSBW delay lines fabricated for this program used split-finger transducers.

In order to obtain low IL with a SSBW delay line, it is necessary (1) to use long transducers to obtain sufficient coupling, and (2) to keep the transducer-to-transducer spacing as short as possible to minimize propagation losses. The use of split-finger transducers minimizes the reflected signals that

TABLE 2-1

SUMMARY OF SSBW DEVICES

Device No.	Cut Angle	Photo-Mask	Temp Sens	Oil Immer	Strain Sensitivity Cyl	Cant	Ten	Comments
B-127	-35	SSBW 5		X				angle cut
B-131	-35	SSBW 6			X			
B-132	-35	SSBW 5	X		X	X	X	
B-133	-35	SSBW 7		X	X			notched, w & w/o oil
B-135	-35	SSBW 5			X	X		angle cut cantilever
B-136	-35	SSBW 7			X			
B-144	-35	SSBW 8		X				angle cut
B-145	-35	SSBW 8	X		X	X		
B-146	-35	SSBW 9				X	X	
B-147	-35	SSBW 9	X	X				
B-148	-35	SSBW 10	X			X	X	
B-149	-35	SSBW 10		X	X			
B-193	-35	SSBW 12						IL vs length
B-194	-35	SSBW 12						IL vs length
B-160	-36	SSBW 5	X			X	X	
B-161	-36	SSBW 5	X					angle cut
B-162	+50.5	SSBW 5	X					angle cut
B-163	+50.5	SSBW 5	X					
B-166	+50.5	SSBW 5				X	X	
B-167	+50.5	SSBW 5			X	X	X	
B-172	+50.5	SSBW 5						accelerometer
B-173	+50.5	SSBW 5			X			
B-174	+50.5	SSBW 5	X					angle cut
B-175	+50.5	SSBW 5						accelerometer
B-177	+50.5	SSBW 5						
B-178	+50.5	SSBW 5		X				
B-179	+50.5	SSBW 5			X	X		
B-182	+50.5	SSBW 5		X				
B-183	+50.5	SSBW 5						recessed trans
B-184	+50.5	SSBW 11						accelerometer
B-186	+50.5	SSBW 11						accelerometer
B-187	+50.5	SSBW 11						accelerometer
B-189	+50.5	SSBW 11						accelerometer
B-190	+50.5	SSBW 11						accelerometer
B-191	+50.5	SSBW 8				X		
B-195	+50.5	SSBW 12						IL vs length
B-196	+50.5	SSBW 12						IL vs length
B-197	+50.5	SSBW 5						accelerometer
B-199	+50.5	SSBW 5						accelerometer

would otherwise be a problem with long transducers, but this design does not, in its simplest form, solve the problem of radiative coupling between input and output transducers that exists when the transducer-to-transducer spacing is small. A modified split-finger design, one that has been used at UTRC in high frequency (>1 GHz) SAW work, was found to be very effective in minimizing radiative coupling in SSBW delay lines. In this newer transducer design, called a co-planar feed transducer, the transducer aperture is split into two equal width portions with parallel electrical inputs as shown in Fig. 2-2. Figures 2-3 and 2-4 show photographs of the photomasks used to generate 24 micron and 48 micron wavelength SSBW delay lines. This co-planar design also makes it possible to minimize the losses resulting from long wire leads between the rf-connector and the delay line pattern on the substrate. In 2-1 the co-planar design, the electrical lead-in lines are designed to have a 50 ohm characteristic impedance and can be brought right to the edge of the quartz substrate, reducing bonding wire lengths to a minimum and thus reducing losses.

Table 2-2 lists the parameters of the photomasks used during AFOSR2. The bulk of the work was done with patterns which had SSBW transducers 200 λ long with 50 λ apertures. The 200 λ length was an estimate of the optimum length. It was also desired to maintain the same geometry for each of the four wavelengths used (24, 32, 40, and 48 microns), and to keep the longest pattern to a total length of about 20 mm so that it could be used on a standard one inch square quartz substrate. The 50 λ aperture was established by the desire to have nearly equal IL values at the fundamental and third harmonic frequencies. The resulting IL values were typically 28 to 32 dB for AT-cut devices and 34 to 37 dB for BT-cut devices.

The optimum length for a SSBW transducer was determined experimentally by fabricating delay lines with 100, 150, 200, and 250 λ transducers on the same substrate and measuring the IL for each device. The aperture of each delay line was adjusted so that the different transducer lengths yielded the same capacitive reactance ($\sim -j50$ ohms) at the fundamental frequency. In this way the IL values could be compared directly without the necessity of correcting for different impedance values. The results of this experiment are shown in Fig. 2-5. Theoretically, in the absence of propagation losses, the IL should continue to decrease with increasing transducer length. However, as the length of the transducer is increased beyond about 216 λ, propagation losses increase faster than than than the increase in acoustoelectric coupling and the overall IL increases. The 200 λ long by 50 λ aperture transducers used for most of the work during this program were therefore quite close to being optimum. Only a small length or aperture correction would be required to bring the capacitive reactance at the fundamental frequency to $-j50$ ohms and reduce the untuned IL of SSBW's on BT-cut quartz a minimum of between 30 and 31 dB.

TABLE 2-2

PARAMETERS OF PHOTOMASKS

Mask Name	Wavelength (microns)	Length (λ)	Aperture (λ)	T-T Separation (λ)	Co-planer Design
SSBW 5	24	200	50	10	yes
SSBW 7	40	150	50	10	yes
SSBW 8	32	200	50	10	yes
SSBW 9	40	200	50	10	yes
SSBW 10	48	200	50	10	yes
SSBW 11	24	250	50	10	yes
SSBW 12	24	100	117.5	10	yes
		150	78.3	10	yes
		200	58.3	10	yes
		250	46.7	10	yes

2.3 Strain Sensitivity

The three loading configurations illustrated in Fig. 2-6 were used to experimentally determine the strain sensitivity of SSBW devices. Cylindrical bending, Fig. 2-6a, in which equal and opposite bending moments are applied to opposite edges of the substrate, results in a uniform bending stress over the middle portion of the substrate. If the substrate's width is two or more times the distance between the central loading pins, as was the case in the UTRC experiments, the perpendicular component of bending stress is small enough to be neglected. As a result, the bending stress at the surface of the substrate has but one component and the analysis of the cylindrical bending experiments is straightforward.

The cantilever bending configuration illustrated in Fig. 2-6b produced the most consistent, repeatable results. The stress in this case varies linearly across the width of the SSBW transducer and so an average value was used in the strain sensitivity computations. Since the SSBW sensors envisioned at this point are based upon the sensitivity of SSBW devices to bending strains, the results of strain experiments using the above two loading configurations are particularly germane.

The straight tension loading configuration illustrated in Fig. 2-6c was employed because, of the three loading configurations, tension loading is the only one that produces a uniform stress throughout the thickness of the substrate. The bending stresses produced by the other two configurations vary with depth into the substrate. Tension loading experiments with brittle materials such as quartz are difficult to implement. The brittle material cannot yield to compensate for even a minute misallignment between the axis of the load and the centerline of the crystal, and significant errors result from the bending stresses generated by the misalignment. Nevertheless, the results of the tension experiments proved to be useful in corroborating the sensitivities obtained from the other loading configurations. Figure 2-7 is a photograph of one of the quartz SSBW substrates epoxy-bonded to aluminum brackets for use in the cantilever bending and tension experiments.

Table 2-3 provides a summary of the strain sensitivity measurements and Fig 2-8 shows the strain sensitivity values plotted versus substrate thickness-to-wavelength-ratio for both AT-cut and BT-cut quartz samples. The loading configuration is indicated in the figure by different data point symbols. A sensitivity of +0.98 ppm/microstrain was obtained for strains perpendicular to the direction of SSBW propagation (transverse sensitivity) on AT-cut samples. This sensitivity agrees well with values obtained previously (Ref. 1). There is, however, no clear dependence upon frequency as was indicated by earlier measurements. The transverse strain sensitivity has now been measured on a sufficient number of AT-cut devices, with frequencies ranging from 128 MHz to 638 MHz, to insure that there is no significant frequency dependence. The parallel strain

TABLE 2-3

SSBW STRAIN SENSITIVITY MEASUREMENTS

Device No	Wavelength (microns)	Thickness h(mm)	h/λ ratio	Loading Configuration: Cylindrical Bending γ_1^{-1} (Units of ppm/microstrain)	Cylindrical Bending γ_2	Cantilever Bending γ_1^{-1}	Cantilever Bending γ_2	Tension γ_2
AT-Cut Devices								
B-131	10.7	0.906	84.7		0.95			
B-132	24	0.901	37.5		1.32			
	8		112.6	-.11	0.91		0.96	0.70
B-133	13.3	0.906	68.1		0.94			
	40		22.7		0.92 (substrate notched)			
	40		22.7		0.89 (notched with oil)			
B-135	24	0.894	37.3		0.94			
	8		111.8		1.02			
	24		37.3				1.10 (beam angled)	
B-136	13.3	0.898	67.5		0.99			
B-145	10.7	0.902	84.3				1.05	0.85
B-146	13.3	0.914	68.7				1.03	
B-148	16	0.904	56.5				1.11	1.21
B-149	16	0.910	56.9		1.05			
B-160	8	0.845	105.6				0.93	1.03
BT-Cut Devices								
B-166	8	0.874	109.3				-1.92	-2.22
B-167	8	0.871	108.9	1.93	-1.89		-2.01	-1.71
B-173	8	0.881	110.1		-1.89			
					-1.89 (w/oil)			
B-176	8	0.875	109.4	1.72	-1.90		-2.03	
	24		36.5	1.61	-1.85		-2.00	
B-179	8	0.876	109.5	1.73	-1.96			
	24		36.5	1.68	-1.54	1.74	-1.73	
B-191	10.7	0.904	84.5				-2.07	
	32		28.2				-1.59	

sensitivity was measured on one AT-cut sample and found to be low (~ 0.1 ppm/microstrain) as previously reported in Ref.1.

The transverse strain sensitivity of the BT-cut devices is also shown in Fig. 2-8. This sensitivity is -1.95 ppm/microstrain and is therefore twice as large as that of AT-cut devices. This high value makes the BT-cut particularly attractive for sensor work. The parallel strain sensitivity of BT-cut quartz is also high with a value of +1.80 as seen in Fig. 2-8.

2.4 Temperature Sensitivity

Figure 2-9 illustrates the calculated first-order temperature coefficient of delay (Tc) at 25°C for SSBW on rotated Y-cut quartz (Ref. 3). For sensor applications, the regions where zero first order Tc exists are the only regions of real interest. The Tc is zero in the vicinity of the AT-cut (-35°), and the BT-cut (+50.5°). Figures 2-10, 2-11, and 2-12 show experimental temperature sensitivity data and parabolic fits for three samples with rotated Y-cut angles of -35°, -36°, and +50.5°. The second order Tc is about 0.06 ppm/°C^2 for the -35° and -36° cuts, and 0.03 ppm/C^2 for the +50.5° cut. The overall temperature sensitivity of the BT-cut is therefore lower than that of the AT-cut. Table 2-4 is a summary of the temperature runs, and Fig. 2-13 is an illustration showing a comparison between the AT and BT-cuts for SSBW and the well known ST-cut for SAW. The SSBW in BT-cut is seen to have the lowest temperature sensitivity of the three. With a second order Tc of 0.03 ppm/°C^2, a SSBW device on BT-cut quartz that can be temperature regulated to within ±1°C will have an accuracy of 0.03 ppm.

There are doubly rotated Y-cut quartz substrates with a zero first order Tc for SSBW's. These cuts posess no clear advantage over the singly rotated cuts as far as temperature compensation is concerned, and they have been studied primarily in an effort to uncover crystallographic orientations with mechanical stress-compensating effects so as to reduce strain sensitivities (Ref. 4). As a result, doubly rotated cuts have not been pursued by UTRC in sensor related work.

2.5 Fluid Immersion Tests

Experiments were conducted to determine the increase in IL of SSBW devices due to fluid loading. The IL of four devices, one each of the 24, 32, 40, and 48 micron wavelength delay line patterns, was recorded and then the entire substrate was immersed in a silicone oil and the change in IL recorded. Table 2-5 summarizes the results of these experiments. For wavelengths 24 microns and longer, the additional loss was 5.8 dB or less. For wavelengths 16 microns and shorter the losses were all above 10 dB. Figure 2-14 thru 2-17 show the effects of oil immersion on 24, 32, 40, and 48 micron wavelength devices respectively.

TABLE 2-4

SUMMARY OF TEMPERATURE TESTING

Device Number	Substrate Cut Angle	Turnover Temperature (°C)	Second Order Coefficient (ppm/°C^2)
B-132	-35°07'	-1.4	0.064
B-145	-34°56'	-3.7	0.071
B-147	-34°58'	-0.9	0.079
B-148	-34°50'	-7.1	0.071
B-160	-35°50'	25.1	0.058
B-161	-35°50'	19.9	0.053
B-162	50°30'	37.3	0.013
B-163	50°30'	40.2	0.023
B-174	50°25'	40.6	0.030

Note: Each value of turnover temperature and second order coefficient represents an average value obtained on several runs with the same device.

TABLE 2-5

SUMMARY OF OIL IMMERSION EXPERIMENTS

Device No.	Wavelength (microns)	Mask Name	IL(init) (dB)	IL(in oil) (dB)	Δ(IL) (dB)
B-149	48.0	SSBW 10	32.5	37.7	5.2
B-147	40.0	SSBW 9	32.9	38.4	5.5
B-144	32.0	SSBW 8	30.4	35.8	5.4
B-127	24.0	SSBW 5	28.1	33.9	5.8
B-149	16.0	SSBW 10	34.6	45.2	10.6
B-147	13.3	SSBW 9	33.7	48.6	14.9
B-144	10.7	SSBW 8	30.5	45.0	14.5
B-127	8.0	SSBW 5	30.6	49.0	18.4

Also note, particularly in the fundamental frequency response of the 24 micron device, the smoothing of the IL response characteristic when the device is immersed in the oil. The oil is effective in damping out extraneous acoustic modes and in reducing radiative feed-through and thus reduces interference with the principle SSBW mode.

SURFACE SKIMMING BULK WAVE RADIATION PATTERN

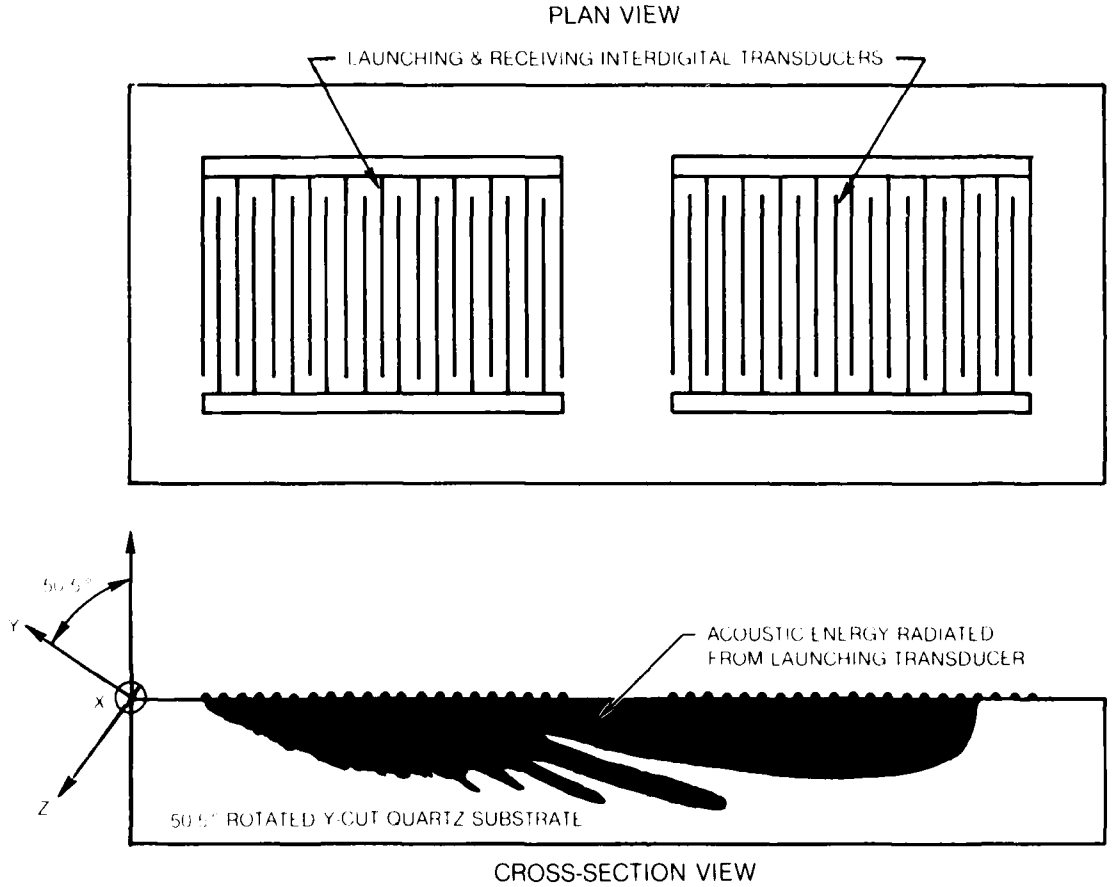

83-4-34-3

FIG. 2-2

CO-PLANAR FEED SSBW DELAY LINE

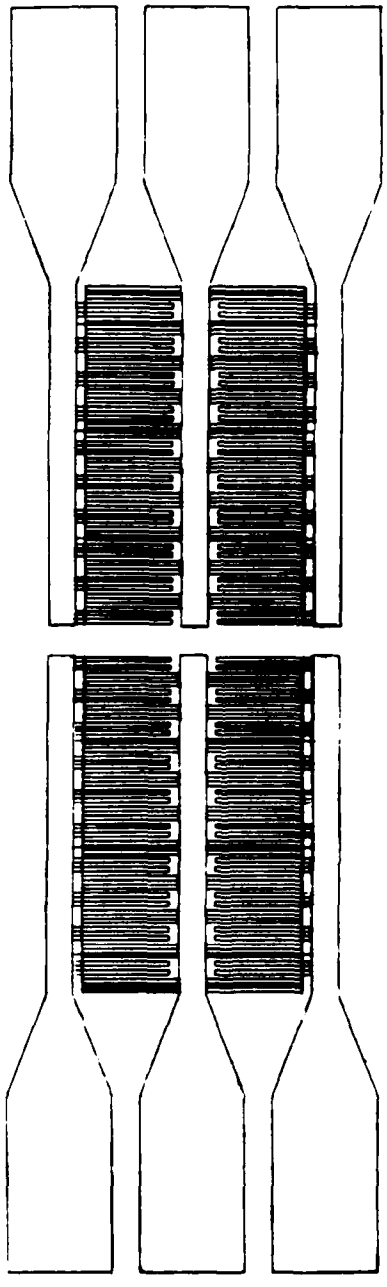

84-9-31-3

FIG. 2-3

SSBW 5

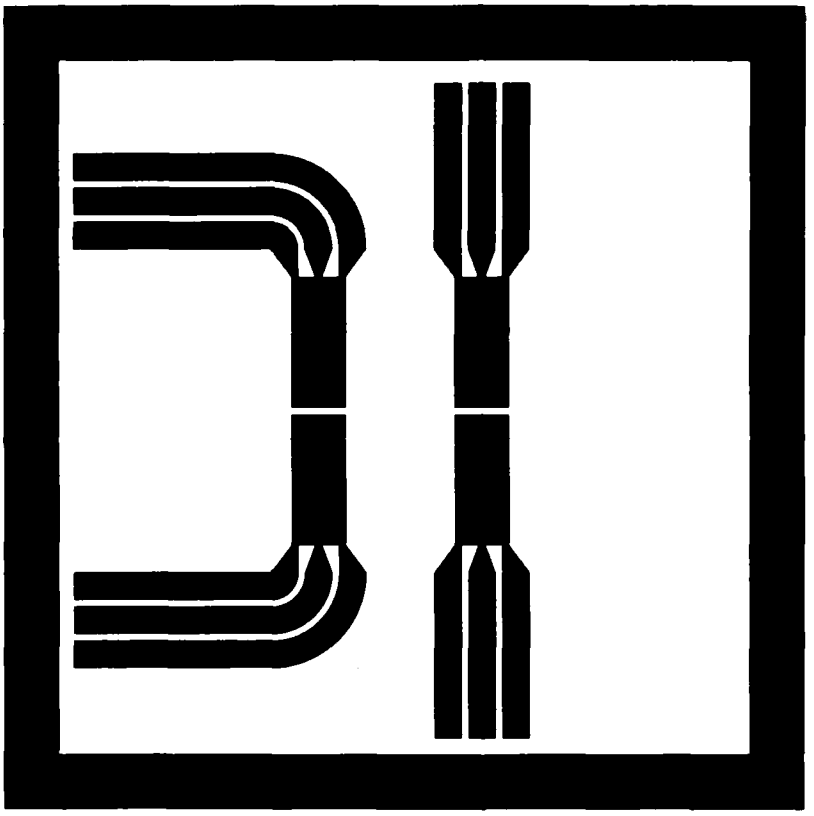

UNITED
TECHNOLOGIES
RESEARCH
CENTER

84-9-31-5

FIG. 2-4

SSBW 10

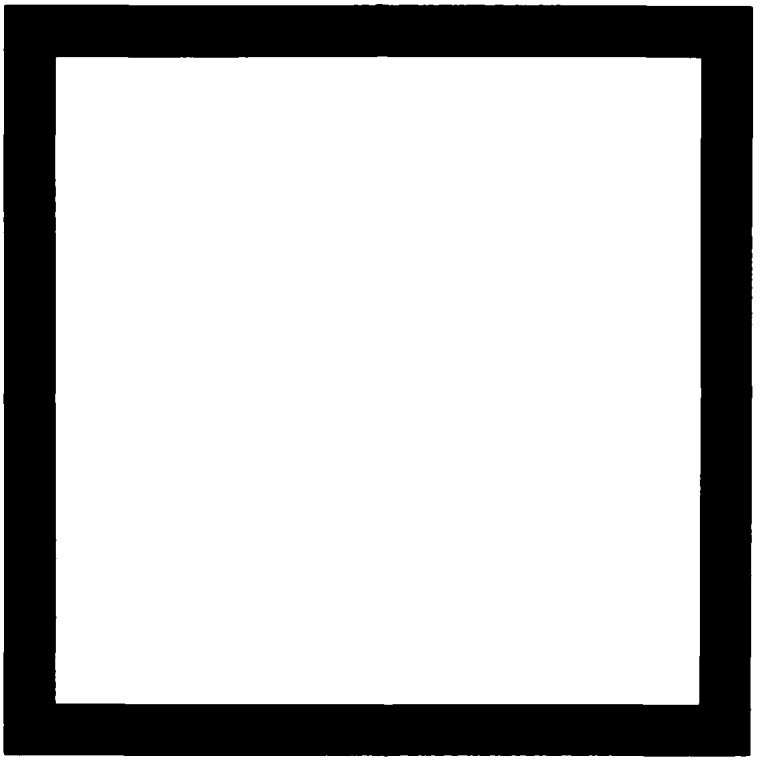

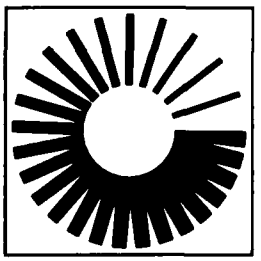

UNITED
TECHNOLOGIES
RESEARCH
CENTER

FIG. 2-5

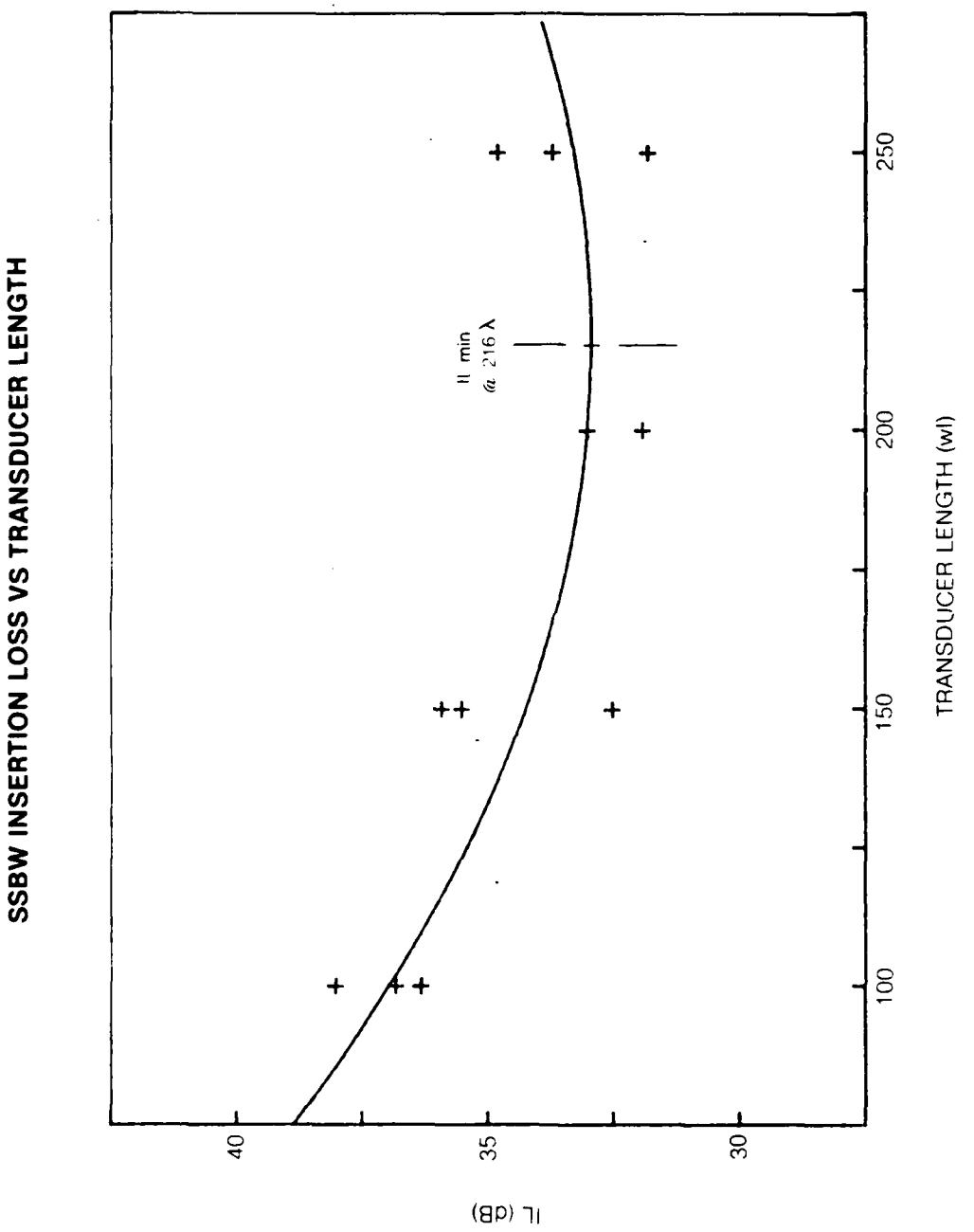

85-1-28-11

LOADING CONFIGURATIONS FOR SSBW STRAIN MEASUREMENTS

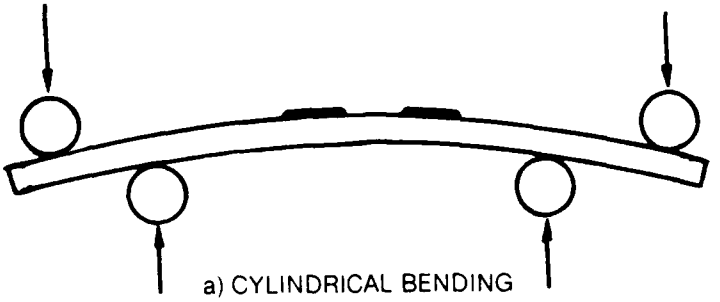

a) CYLINDRICAL BENDING

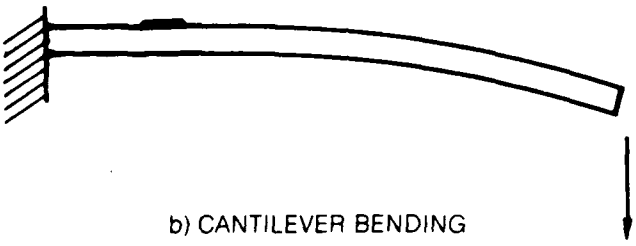

b) CANTILEVER BENDING

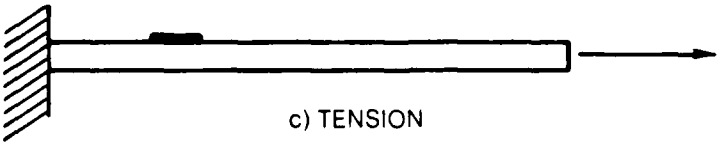

c) TENSION

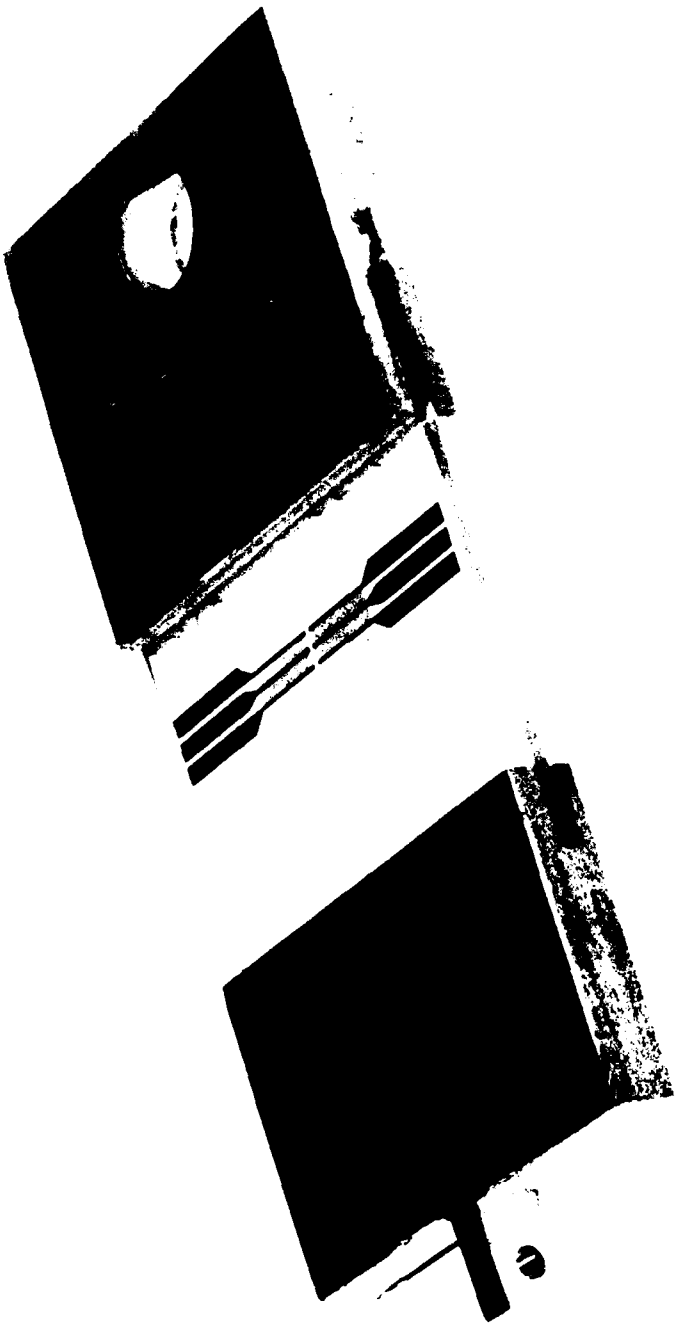

SSBW SUBSTRATE MOUNTED FOR STRAIN EXPERIMENTS

SSBW STRAIN SENSITIVITY

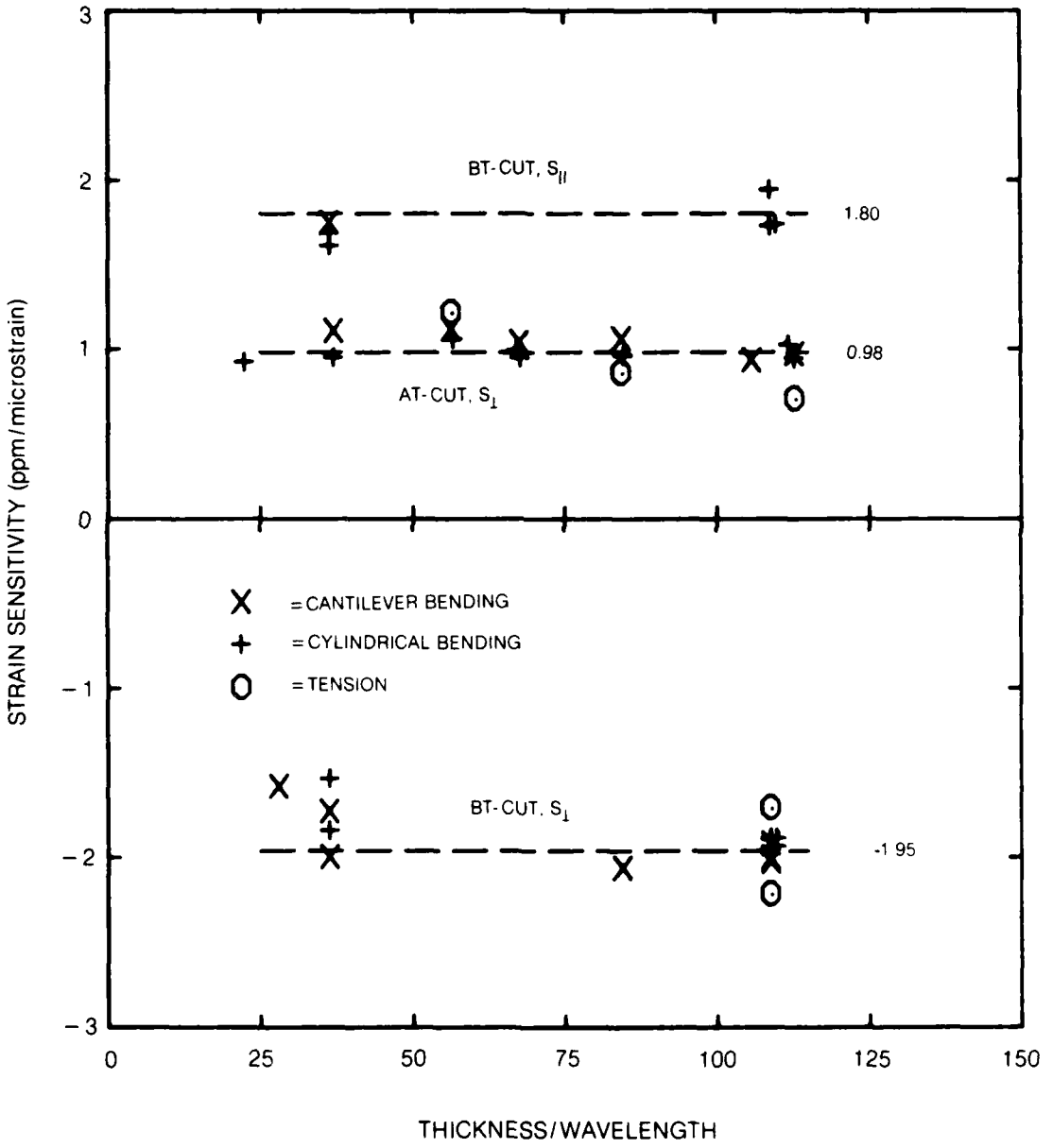

85-1-28-4

FIRST-ORDER TEMPERATURE COEFFICIENT OF DELAY OF SSBW IN ROTATED Y-CUT QUARTZ

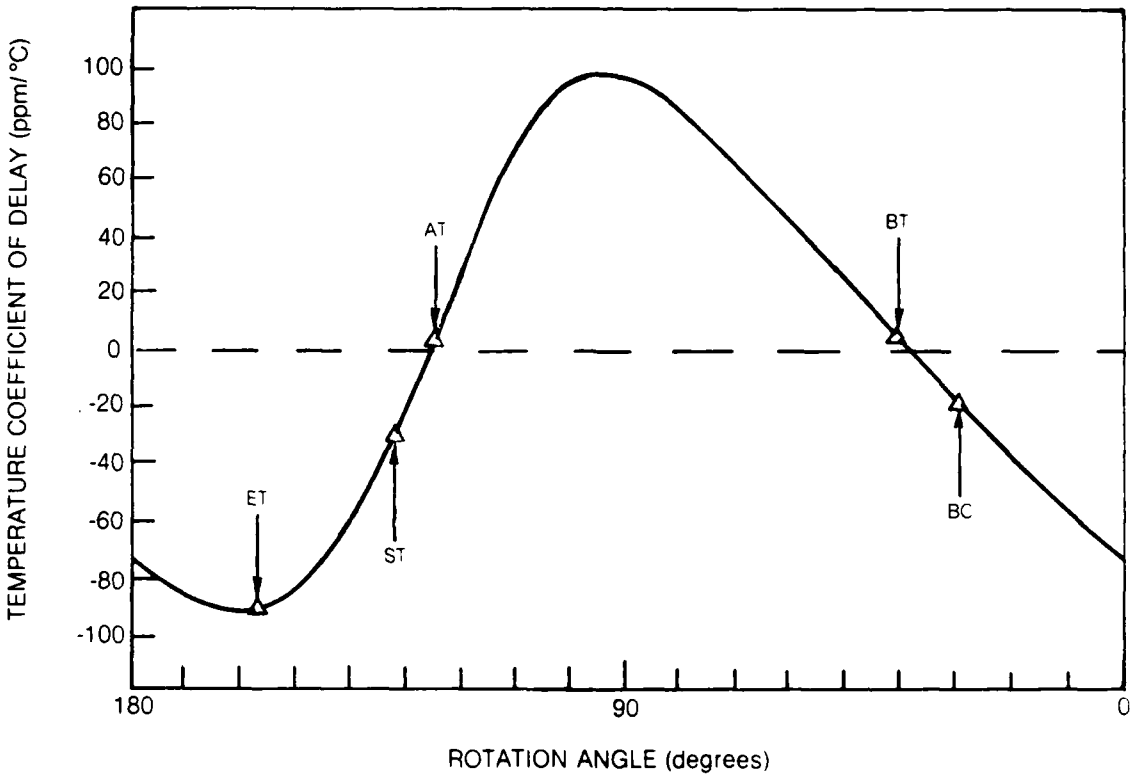

84-9-31-2

SSBW TEMPERATURE SENSITIVITY

-35° ROTATED Y—CUT QUARTZ

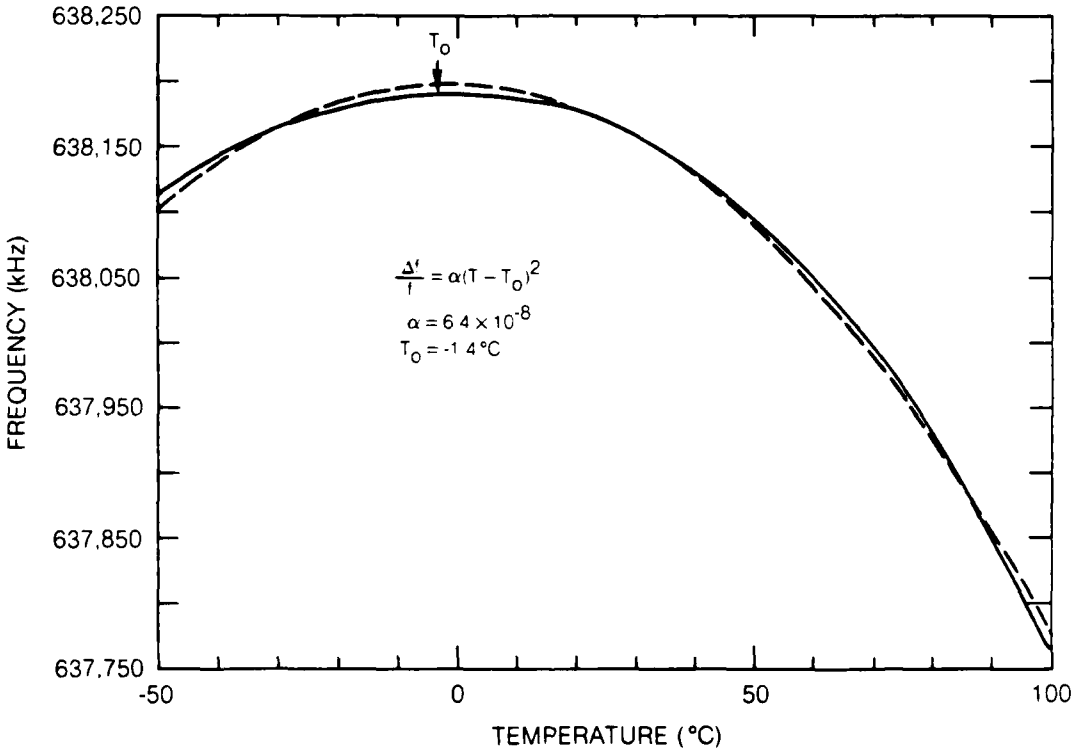

84-7-66-7

FIG. 2-11

SSBW TEMPERATURE SENSITIVITY

-36° ROTATED Y—CUT QUARTZ

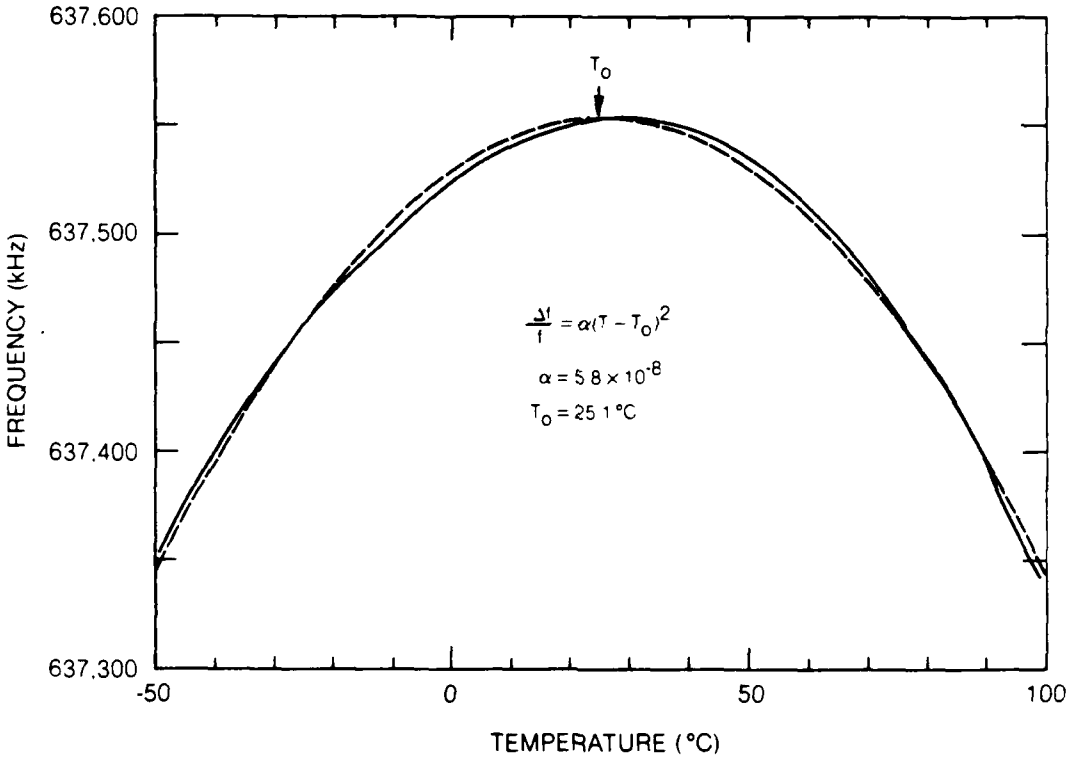

84-7-66-8

FIG. 2-12

SSBW TEMPERATURE SENSITIVITY

+ 50.5° ROTATED Y—CUT QUARTZ

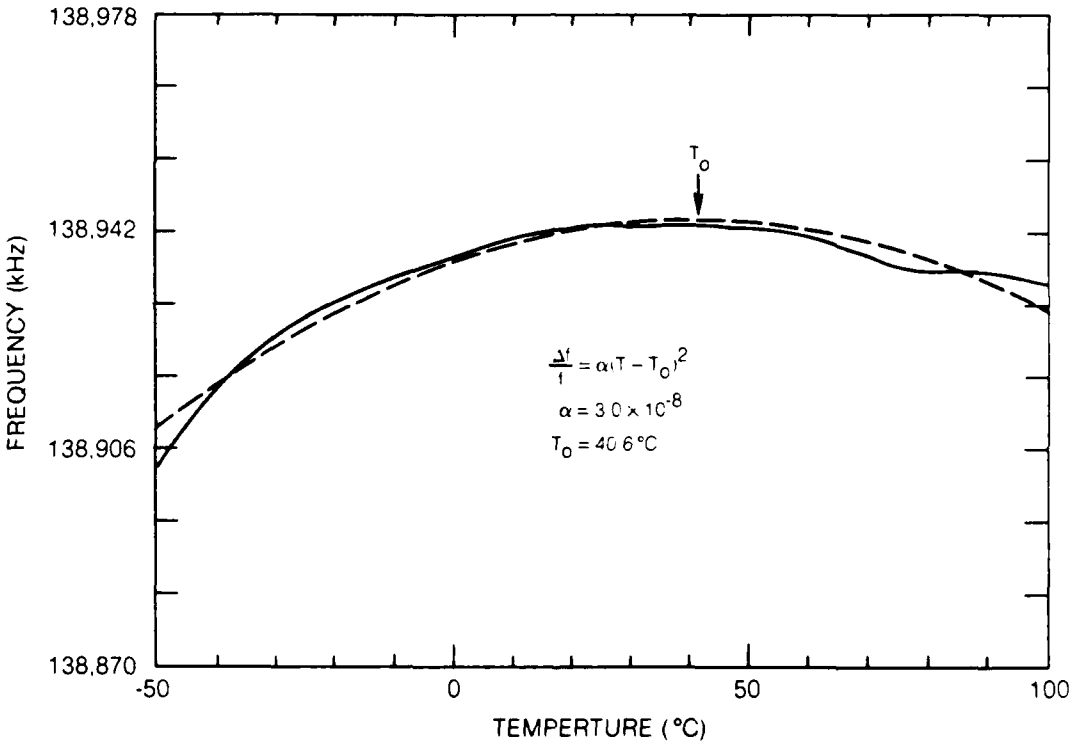

84-7-66-9

COMPARISON OF TEMPERATURE SENSITIVITIES

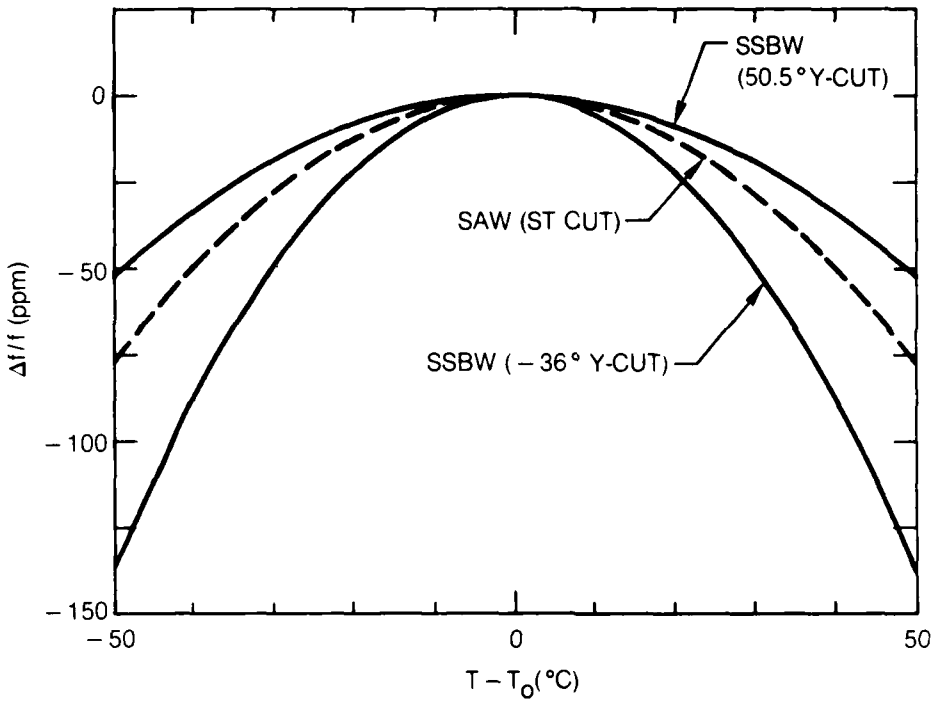

84-7-66-6

FIG. 2-14

EFFECTS OF OIL IMMERSION ON $\lambda = 24\mu$ SSBW CHARACTERISTICS

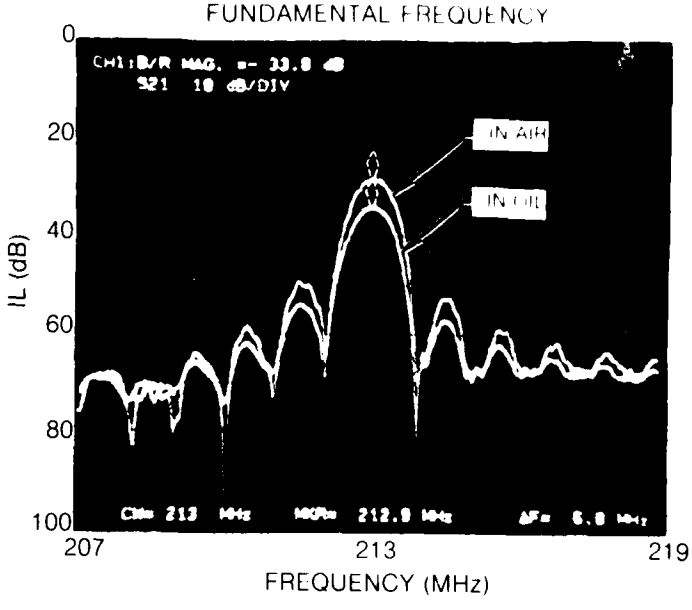

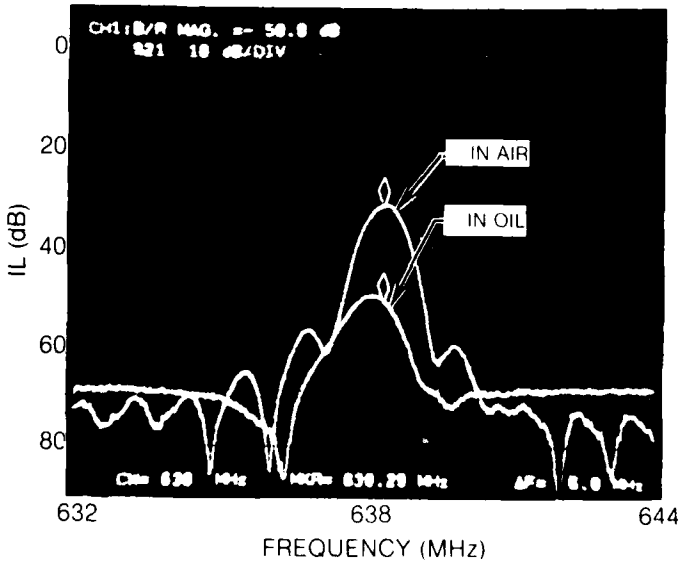

84-7-66-2

FIG. 2-15

EFFECTS OF OIL IMMERSION ON $\lambda = 32\mu$ SSBW CHARACTERISTICS

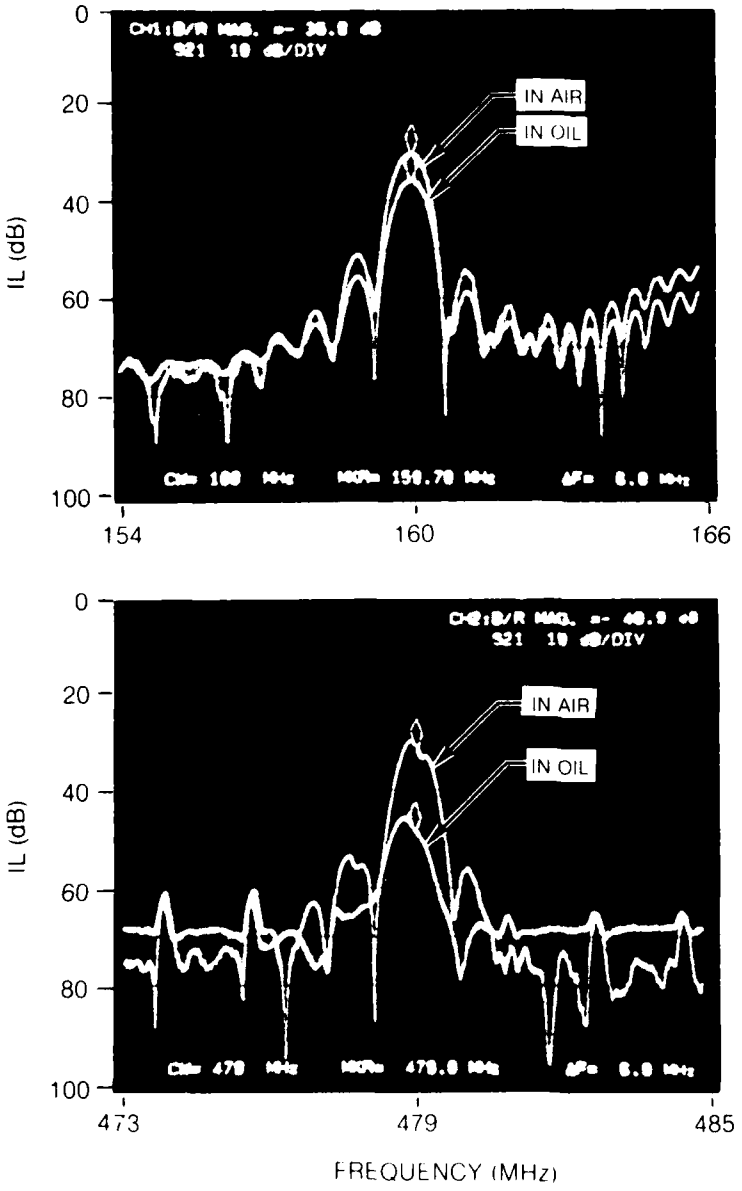

85-1-28-3

FIG. 2-16

EFFECTS OF OIL IMMERSION ON $\lambda = 40\mu$ SSBW CHARACTERISTICS

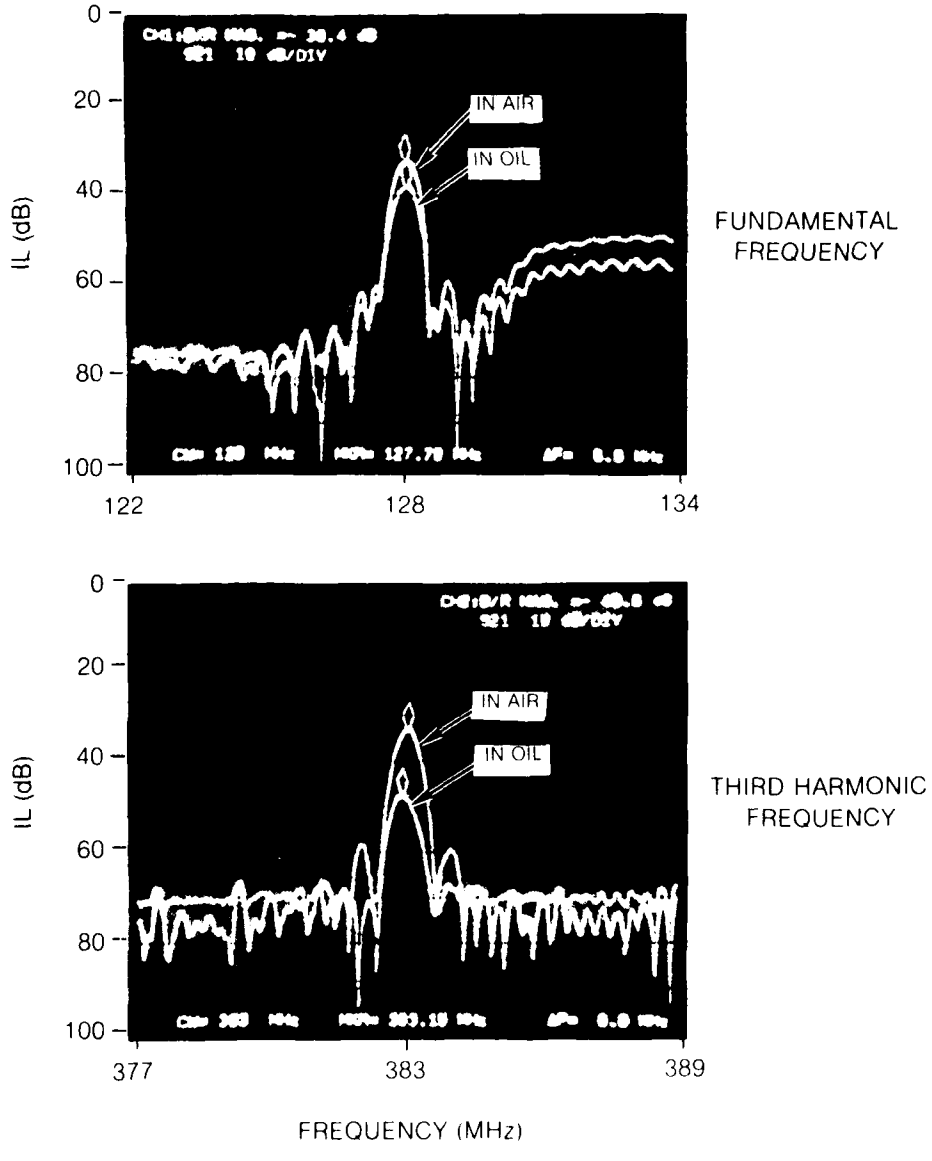

85-1-28-2

FIG. 2-17

EFFECTS OF OIL IMMERSION ON $\lambda = 48\mu$ SSBW CHARACTERISTICS

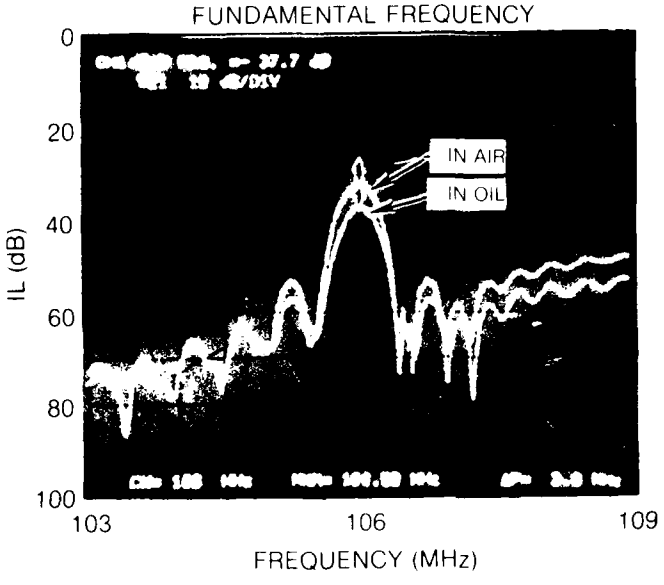

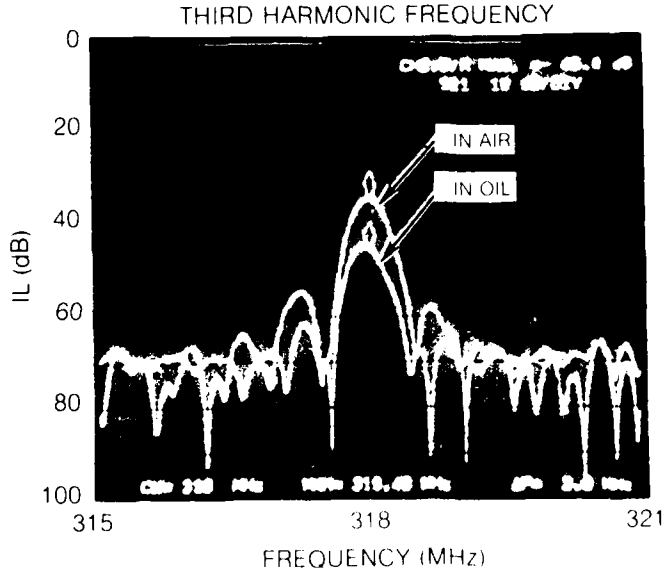

84-7-66-1

3.0 LABORATORY SSBW ACCELEROMETERS

Figure 3-1 illustrates two views of the design from which the laboratory SSBW accelerometer models were constructed. The single SSBW oscillator devices were fabricated on nominal 0.9 mm thick quartz substrates. The sides of the substrates were cut at an angle as shown to prevent reflected signals from interfering with the fundamental frequency SSBW. Figure 3-3 shows the improvement in the IL characteristic when the edges of the substrate were angled. Figure 3-3 is a photograph of one of the angled accelerometer substrates. As described earlier, a further reduction in interfering signals was obtained when the device was immersed in the damping fluid. A 10 to 15 gram tungsten mass was epoxy bonded to the narrow end of the substrate using a small alluminum adapter piece. The substrate, in turn, was epoxy bonded to the brass chassis. The RF connectors are positioned so that the electrodes lie close to the co-planar feed lines of the transducers. The ends of the feed lines were plated with copper so that the electrical connections could be made by soldering gold ribbons between the feed lines and the RF connector electrodes. In this way the interconnections were made very rugged and could withstand repeated immersions in oil and the cleaning with solvents that followed. Figure 3-4 is a photograph of one of the experimental accelerometers.

Table 3-1 shows the relevant parameters and the calculated and measured acceleration sensitivities of four of the laboratory accelerometers built and tested. All of these devices were made using BT-cut quartz. The experimental strain sensitivity values (γ_1-1 = 1.80, γ_2 = -1.95) were used to obtain the calculated acceleration sensitivities. The analytical values were arrived at by first determining the bending stress at the SSBW device position due to a 1G acceleration from the relation

$$T_{\perp} = 6*m*G*l/w*h^2$$

and the associated strain from the relation

$$S_{\perp} = T_{\perp}/C^*_{\parallel}$$

where $C^*_{\parallel}$ is the appropriate element of the C matrix for the BT-cut quartz plate ($C^*_{\parallel}$ = 12.6x10^6 psi). It is assumed that $T_{\perp}$ and $S_{\perp}$ are the only significant components of stress and strain. Finally the acceleration sensitivity, η_a, in units of ppm/G is obtained from

$$\eta_a = \gamma 2 * S_\perp$$

Sensitivities in units of KHz/G are obtained by multiplying by the frequency(in MHz) and dividing by 1000, i.e.,

$$\eta_a \text{ (KHz/G)} = \eta_a \text{(ppm/G)} * f\text{(MHz)}/1000.$$

This analysis is capable of predicting the acceleration sensitivity to within a few percent as seen in Table 3-1.

In order to be able to assess the significance of the acceleration sensitivity values obtained here, it is necessary to look at the degree of temperature compensation the can be obtained with these devices, and to know what level of long term stability, or aging, can be achieved with present day SSBW devices. In Section 2 it was shown that SSBW's on BT-cut quartz have zero first order and 0.03 ppm/°C second order temperature coefficients. As discussed in Section 3.4, this means that, if the temperature can be controlled to within +1°C of the operating temperature, then the maximum error due to temperature fluctuations within that 13C range will be 0.03 ppm. If the accelerometer has an acceleration sensitivity of 30 ppm/G, then the maximum acceleration error will be (0.03 ppm)/(30 ppm/G) = 0.001 G. Hence, even with the laboratory SSBW oscillator accelerometer that presently exists, resolution of accelerations as small as 1 milli-G are already possible. More sophisticated devices, using dual SSBW oscillators, will therefore be able to achieve resolutions well below 1 milli-G. Table 3-2 presents a comparison between the sensitivity of the present day laboratory SSBW accelerometer and the performance projected for the next generation dual-oscillator SSBW accelerometers. This next generation of devices would use two SSBW oscillators on opposite sides of the same substrate to double the acceleration sensitivity while, at the same time, significantly reducing the temperature sensitivity. By mixing the two oscillator frequencies and taking the difference frequency output, temperature effects are largely cancelled because they drive the oscillators in the same direction, while acceleration effects add because they produce strains that drive the oscillators in opposite directions. Even if the two second order temperature dependencies do not entirely cancell one another, the resulting linear temperature dependence will be small and can be corrected for. As a result, the dual oscillator SSBW accelerometer has excellent potential.

TABLE 3-1

PARAMETERS AND CHARACTERISTICS OF
LABORATORY SSBW ACCELEROMETERS

Sample Number	B-172	B-175	B-197	B-199
Frequency [f] (MHz)	138.7	138.8	138.7	138.7
Mass [m] (grams)	14.2	10.7	13.3	14.7
Beam length [l] (SSBW device to mass) (mm)	20.7	20.6	18.6	20.8
Beam width [w] (@ SSBW device) (mm)	16.3	16.5	15.5	15.5
Beam thickness [h] (mm)	0.880	0.871	0.906	0.909
Acceleration Sensitivities				
Calculated (kHz/G)	4.29	3.23	3.56	4.37
(ppm/G)	30.8	23.3	25.7	31.5
Measured (kHz/G)	4.40	3.21	3.41	4.13
(ppm/G)	31.7	23.1	24.6	29.8
|Calculated - Measured| (%)	2.6	0.6	4.2	5.5

TABLE 3-2

SSWB ACCELEROMETER DEVELOPMENT

	Present Program Results	Projected Dual-Oscillator Performance
Acceleration Sensitivity	30 ppm/G	60 ppm/G
Temperature Sensitivity	0.03 ppm/°C^2	< 0.003 ppm/°C^2
Acceleration Sensitivity Limit (± 1°C temp control)	1 milli-G	< 50 micro-G

The question of SSBW sensor long term stability is largely unknown at this time. The present state-of-the-art ageing rate of SAW devices is approximately 1 ppm/year. Because SSBW's are horizontally polarized shear waves and are not nearly as sensitive to surface effects as are SAW's, experts in the field expect the aging of SSBW devices to be better than that of SAW devices (Ref. 2, 3).

EXPERIMENTAL SSBW ACCELEROMETER

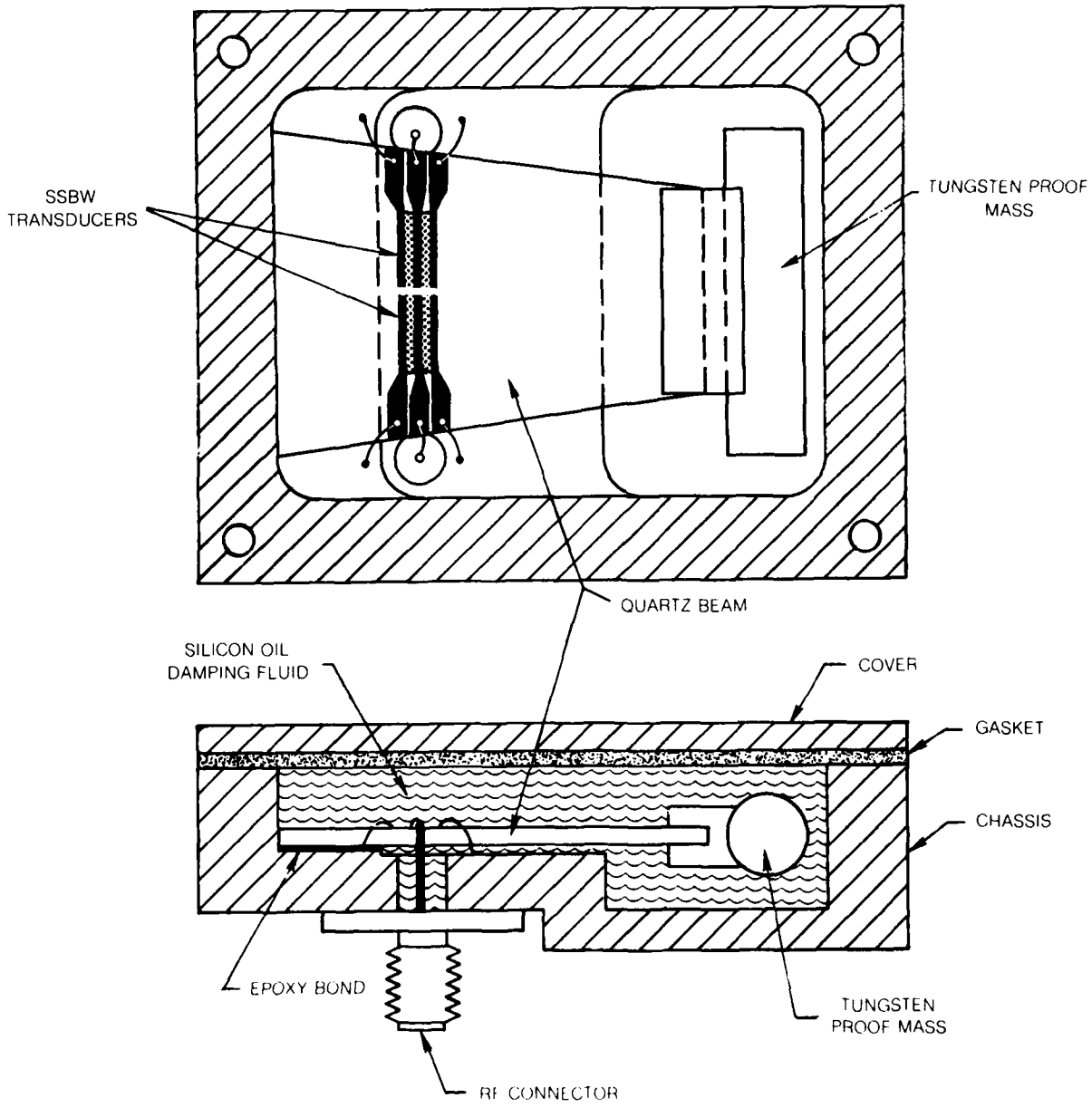

85-1-28-6

R85-926671

SSBW ACCELEROMETER SUBSTRATE

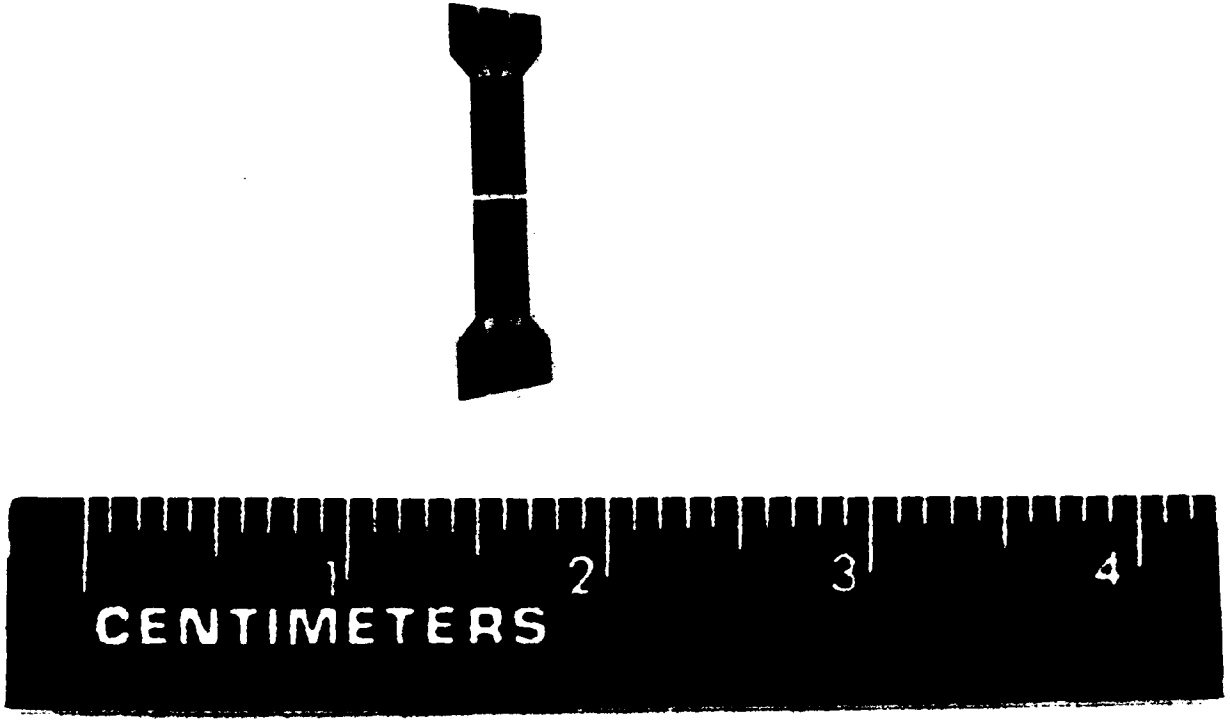

85-1-28-9

FIG. 3-2

LABORATORY SSBW ACCELEROMETER

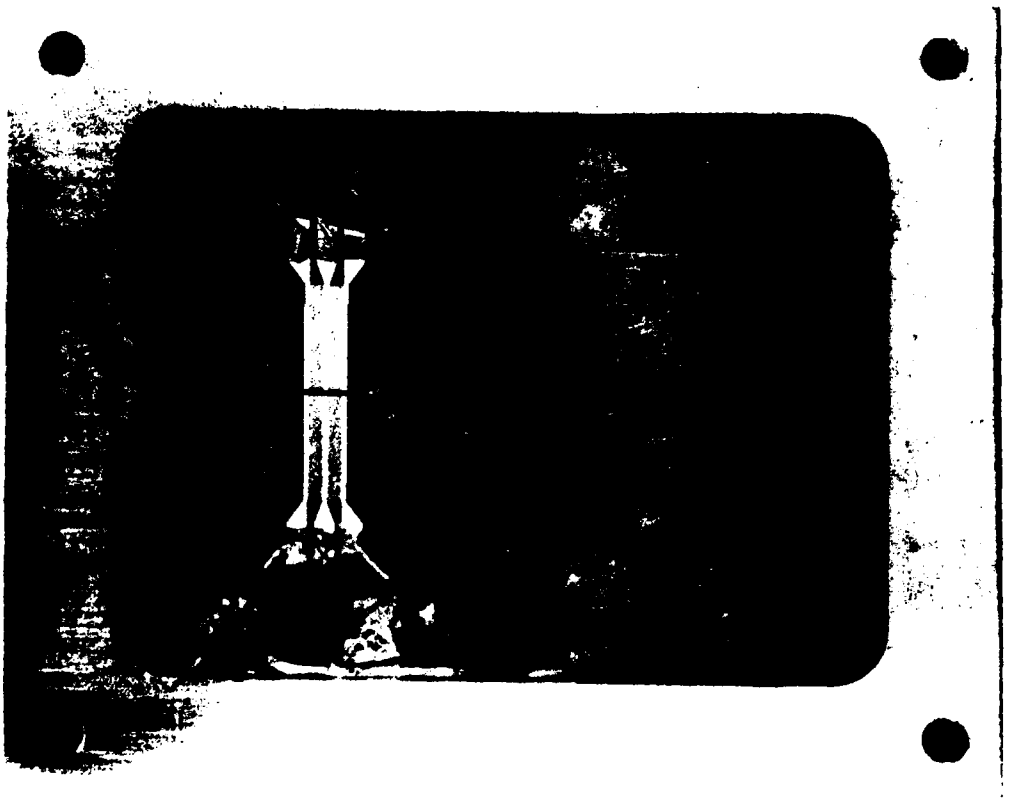

85-1-28-10

REDUCTION OF INTERFERENCE EFFECTS DUE TO ACOUSTIC REFLECTIONS

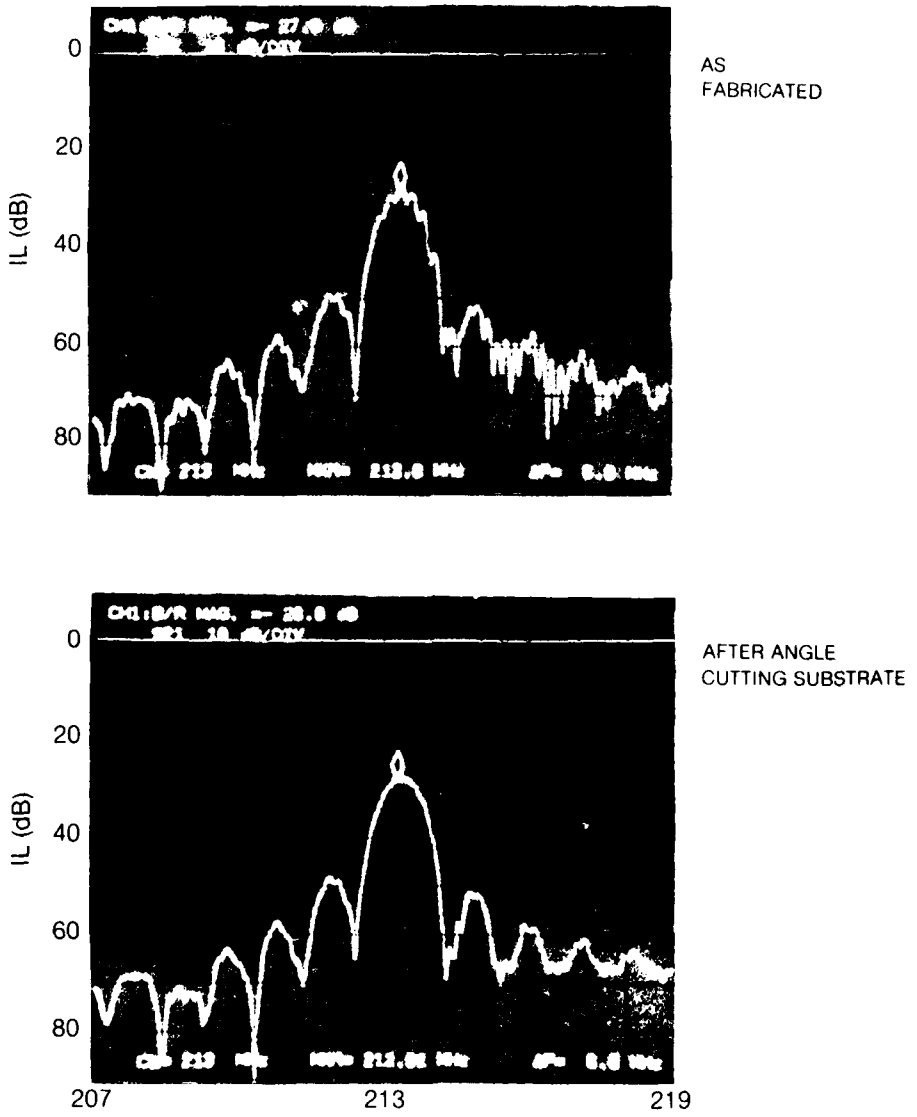

84-7-66-4

4.0 SUMMARY AND RECOMMENDATIONS FOR CONTINUED DEVELOPMENT

The SSBW in BT-cut quartz has outstanding potential for acoustic sensor development. With a strain sensitivity of 2 ppm/microstrain, zero first order and 0.03ppm/$^{\circ}C^2$ second order temperature coefficients, and 6 dB or less attenuation due to surface fluid loading, this acoustic mode is a very attractive candidate for sensor applications. Several aspects of SSBW device performance that relate directly to SSBW sensor development have yet to be addressed.

The most important of the issues yet to be resolved is that of the long-term stability or ageing of SSBW devices, and particularly the ageing of devices in a fluid environment. It is necessary to address this aging question by fabricating SSBW devices using techniques known to produce the lowest ageing SAW devices and to monitor their performance in oscillator circuits for a period of at least one year. A portion of the SSBW devices should be vacuum encapsulated to determine a base line ageing rate, while the remainder should be immersed in silicone oil for the duration of the test period to access the aging performance under such conditions. Since a practical SSBW accelerometer prototype would use a pair of SSBW devices on a single substrate to achieve a higher level of performance, the aging tests should be performed with pairs of SSBW devices fabricated on the same substrate to ascertain the possible benefits of pair aging.

Earlier developmental work on SAW pressure transducers has shown that a dual oscillator configuration, were two SAW devices were fabricated on a single quartz substrate, can double the pressure (i.e. strain) sensitivity of the sensor while reducing the temperature sensitivity by more than two orders of magnitude. This same type of dual oscillator design can be employed with SSBW devices with similar increases predicted in sensor performance. Before a dual oscillator SSBW sensor can be designed however, the question of how closely the SSBW devices can be positioned without frequency locking needs to be resolved experimentally, and techniques need to be developed for fabricating SSBW devices on opposite sides of the same substrate. Also, the mechanical design of a prototype cantilever beam SSBW accelerometer requires a knowledge of the damping and vibration characteristics of the cantilevered quartz beam in a fluid environment. A straightforward experimental research effort using advanced fabrication, design, and measurement techniques is envisioned, resulting in a prototype SSBW accelerometer with better than 1 milli-G sensitivity and resolution.

5.0 REFERENCES

1. Cullen, D.E., G. Meltz and T.W. Grudkowski: Research and Development of Subsurface Acoustic Wave Device Configurations for Sensor Applications. Final Report on AFOSR Contract No. F49620-82-C-0074, September 1983.

2. Lewis, M.: Surface Skimming Bulk Waves. Proc. 1977 IEEE Ultrasonics Symposium, 744(1977).

3. Yen, K.H., K.G. Lau and R.S. Kagiwadw: Recent Advances in Shallow Bulk Acoustic Wave Devices. Proc. 1979 IEEE Ultrasonics Symposium, 776(1979).

4. Cullen, D.E., G. Meltz and T. W. Grudkowski: Surface and Interface Acoustic Waves in SiO_2/YX-$LiNbO_3$. Appl. Phys. Lett. 44, 182(1984).

5. Cullen, D.E. and T.W. Grudkowski: Strain Sensitivity of SSBWs In Quartz. Proc. 1984 IEEE Ultrasonics Symposium (to be published).

6.0 PUBLICATIONS AND PRESENTATIONS

6.1 Publications

"Strain Sensitivity of SSBWs In Quartz" by D. E. Cullen and T. W. Grudkowski - to be published in 1984 IEEE Ultrasonic Symposium Proceedings.

6.2 Presentations

"Strain Sensitivities of SSBWs in Quartz" by D. E. Cullen and T. W. Grudkowski - at 1984 IEEE Ultrasonics Symposium in Dallas, Texas on November 16, 1984.

7.0 LIST OF PROFESSIONAL PERSONNEL

Program Manager

T. W. Grudkowski - Manmger, Semiconductor Research Laboratory - Ph.D in Electrial Engineering at Stanford University, 1975 - thesis title "Active Acoustic Waves and Electrons in Gallium Arsenide"

Principal Investigator

D. E. Cullen - Senior Research Scientist, Microelectronics Ph.D. in Physics at the University of Illinois, 1970 thesis titled "Tunneling Spectroscopy in P-Type Silicon"

APPENDIX A

PREPRINT OF PAPER

TO BE PUBLISHED IN

1984 IEEE ULTRASONICS SYMPOSIUM PROCEEDINGS

STRAIN SENSITIVITY OF SSBWS IN QUARTZ*

D. E. Cullen and T. W. Grudkowski
United Technologies Research Center
East Hartford, Ct. 06108

Abstract

The sensitivity of SSBWs to substrate strains has been measured in AT and BT-cut quartz. Using the SSBW delay path in a feedback oscillator network, strain sensitivities were determined from the variations in oscillator frequency with applied load. Three different loading configurations were employed: cylindrical bending, cantilever bending, and uniaxial tension. The effect of applied strains both parallel and transverse to the acoustic propagation path were examined. The application of a strain sensitive SSBW device configuration as a fluid damped, cantilever beam accelerometer is described and experimental results presented.

Introduction

The sensitivity of SSBWs to substrate strains is of interest for two principal reasons. In the design of SSBW devices with high stability requirements, a knowledge of the strain sensitivities will make it possible to minimize output variations due to stresses generated by the mounting and packaging of the device. On the other hand, those interested in developing SSBW sensors will need to be aware of the strain properties in order to be able to maximize strain sensitivity. Because of their desirable temperature properties (Ref. 1), two crystallographic orientations of quartz, the regions near the AT and BT-cuts, are of particular interest for SSBW applications.

The strain sensitivities of AT and BT-cut quartz have been experimentally measured for normal strains both parallel and transverse to the SSBW propagation direction. While loading configurations that produce bending strains were used principally, uniaxial tension experiments were also performed. The results of these experiments were used to design a laboratory model of a fluid-damped, cantilever beam accelerometer. This sensor is described and the measured acceleration sensitivity given and compared to that predicted by the strain sensitivity measurements.

Experimental Methods

The different three loading configurations were employed in this study; cylindrical bending, cantilever bending, and uniaxial tension. Cylindrical bending results in a simple one-component state of strain at the surface of the substrate making interpretation of the experimental results particluarly straightforward (Refs. 2, 3). The cantilever bending experiments produced the most precise frequency versus load data because of the absence of deleterious frictional forces in the loading arrangement and the non-critical nature of the loading geometry. Since the application of a strain sensitive SSBW device

*This work supported by U. S. Air Force (AFOSR) Contract No. F49620-84-C-0006

to an accelerometer or other type of sensor would most likely be based upon sensitivity to bending strains, the results of measurements made with the above two loading configurations are particularly relevant.

The normal strains developed by these bending loads vary linearly throughout the thickness of the substrate with maximum values at the surfaces, one surface in tension and the other in compression. If the substrate thickness, h, is many times the SSBW wavelength, β, then the error incurred by treating the strain as a constant equal to its value at the surface is small. In the present experiments, h = 0.89 mm, and β = 0.008 to 0.048 mm, so that β = 0.9 to 5.4% of h. Shear strains are zero at the surface in the case of cylindrical bending and negligibly small with cantilever loading.

Uniaxial tension experiments were performed to examine the effects of variation in stress with depth into the substrate because, of the three loading configurations, only uniaxial tension produces a uniform stress throughout the thickness of the substrate. Tension loading experiments with brittle materials such as quartz are difficult to implement however. The condition of uniform stress depends upon being able to obtain a very high degree of perfection in the geometry of the loading arrangement because the brittle substrate cannot yield to compensate for even a minute mis-alignment between the axis of the load and the centerline of the crystal. Significant errors can result from the bending stresses generated by any mis-alignment. Nevertheless, the results of the tension experiments proved to be useful in corroborating the sensitivities obtained from the other loading configurations.

Substrates used in this study were either -35.5±0.7 degree rotated Y-cut quartz (AT-cut), or +50.5±0.7 degree rotated Y-cut quartz (BT-cut). SSBW transducers were typically 200β long, 50β wide, and input and output transducers were separated by 10β. A co-planar feed transducer design was used to minimize radiative coupling and to bring the bonding pads to the edge of the substrate. Untuned insertion losses were typically 30 to 33 dB for AT-cut devices, and 34 to 36 dB for BT-cut devices.

Strain sensitivity measurements were performed by inserting the SSBW delay line into a feedback oscillator network and recording the variation in oscillator frequency, f, with applied load. The associated strain, S, was determined from the appropriate elasticity relationships. Sample substrates with Micro-Measurements EA-06-031DE-120 strain gages bonded to them were used to confirm the relations between applied load and substrate strain. Values of strain sensitivity, $(1/f)(df/dS)$, are given in units of ppm/microstrain (ppm/uS).

Because SSBWs are horizontally polarized shear waves, they are insensitive to surface contamination and, in fact, can exist in a fluid environment. In order to determine the losses due to fluid loading, SSBW delay lines were immersed in a silicone oil and the increase in loss noted. The results of this experiment are particularly relevant to the design of a cantilever beam SSBW accelerometer since the beam must be fluid damped in order to achieve both high acceleration sensitivity and an acceptable vibration response characteristic near the mechanical resonance frequency.

Experimental Results

Figure 1 shows the results of the SSBW strain sensitivity measurements plotted as a function of h/β. The data points from the uniaxial tension experiments are included in Fig. 1 for completeness, but are not otherwise used. Strain sensitivity values given below and plotted as dashed lines in Fig. 1 are averages of sensitivities measured for $h/\beta > 60$. The accuracy of

these sensitivity values is estimated, based upon the spread in measured values and the accuracy with which the parameters of the experiment can be determined, to be ±0.09 ppm/uS.

For AT-cut quartz and strain transverse to the acoustic propagation direction, a sensitivity value of 0.98 ppm/uS was observed. AT-cut devices were insensitive to strain parallel to the propagation direction, with all values of sensitivity measured for this configuration found to be less than 0.1 ppm/uS. The magnitude of the SSBW strain sensitivity of BT-cut quartz is higher for both strain orientations. For parallel strain the value is 1.80 ppm/uS. For transverse strain the value is -1.95 ppm/uS, almost exactly twice as large in magnitude as that of AT-cut quartz. The four values of strain sensitivity are summarized in Table 1.

Table 1
SSBW Strain Sensitivities

Substrate Orientation	Parallel (ppm/uS)	Transverse (ppm/uS)
AT-cut	(0.1	0.98
BT-cut	1.80	-1.95

A decrease in strain sensitivity with increasing wavelength is evident in Fig. 1 in the data from the BT-cut samples. This reduction in sensitivity as the h/β ratio decreases is expected on physical grounds and was predicted theoretically for SAWs by Sinha and Tiersten (Ref. 4). The same roll-off in sensitivity is not obvious in the AT-cut data, however significant differences in the dependence upon h/β were predicted for SAWs in Y-cut and ST-cut quartz (Ref. 4) and the same type of mechanism may be responsible for the difference noted here.

Figure 2 is a network analyzer display of insertion loss (IL) versus frequency of a SSBW delay line in air and immersed in a silicone oil. The additional loss due to the fluid loading is ~5 dB. This result is typical of all of the AT-cut and BT-cut delay lines which were examined. Note also that the IL versus f characteristic obtained with the device immersed in oil is smoother than that in air indicating that the oil is effective in absorbing some of the unwanted bulk modes that are generated by the SSBW transducers.

SSBW Accelerometer

With high transverse strain sensitivity (~2 ppm/uS), low temperature sensitivity (zero first order and 0.03 ppm/°C/°C second order temperature coefficients), and low fluid loading losses (~5 dB), the SSBW mode in BT-cut quartz is well suited for use in a fluid damped, cantilever beam accelerometer. The trade-off between sensitivity and the mechanical resonance frequency in the design of a cantilever beam accelerometer requires that the beam be damped in order to realize a practical device. Figure 3 is a drawing of a basic SSBW accelerometer which has been built and tested for acceleration sensitivity and mechanical rsonance behavior. Table 2 gives the relevant parameters of two of these devices along with the calculated and measured acceleration sensitivities.

Table 2
Parameters & Sensitivities
of
Laboratory Accelerometers

Sample Number	B-172	B-175
Frequency (Mhz)	138.7	138.8
Mass (gms)	14.2	10.7
Length (mm)	20.7	20.6
Width (mm)	16.3	16.5
Thickness (mm)	0.880	0.871
Acceleration Sensitivity		
Calculated (khz/G)	4.29	3.23
(ppm/G)	30.9	23.3
Measured (khz/G)	4.40	3.21
(ppm/G)	31.7	23.1

Because opposite sides of the cantilever have strains of opposite sign, the acceleration sensitivity can be doubled from the above values by employing two SSBW delay lines on either side of the beam. If the temperature of the beam can be controlled to ±1.0 °C, then the error due to temperature variation can be held to 0.03 ppm or ~0.5 milli-G assuming a 60 ppm/G sensitivity. This level of acceleration sensitivity is adequate for many applications.

Conclusions

The strain sensitivities of SSBWs in AT and BT-cut quartz have been measured experimentally. The values for the two cuts are found to be quite different with the higher BT-cut values greater than any strain sensitivities measured or predicted for SAWs. If a practical sensor is to be developed utilizing SAW or SSBW technology, the SSBW in BT-cut quartz is clearly a very promising configuration. At the same time, the low sensitivity of SSBWs in AT-cut quartz to parallel strains provides the device engineer with a guide to achieving low mounting strains.

Acknowledgements

It is a pleasure to acknowledge the contribution made by R. Basilica in the preparation and mounting of samples and the assistance of S. Sheades in the experimental measurements.

References

1. Lewis, M.F.: Surface Skimming Bulk Waves, 1977 Ultrasonics Symposium Proceedings, p. 744-752.
2. Cullen, D.E. and T.M. Reeder: Measurement of SAW Velocity Versus Strain for YX and ST Quartz, 1975 Ultrasonics Symposium Proceedings, p. 519-522.
3. Timoshenko, S. and S. Woinowsky-Krieger: Theory of Plates and Shells, McGraw-Hill, 1959.
4. Sinha, B.K. and H.F. Tiersten: On the Influence of a Flexural Biasing State on the Velocity of Piezoelectric Surface Waves, Technical Report No. 24 on ONR Contract No. N00014-76-C-0368, April 1978.

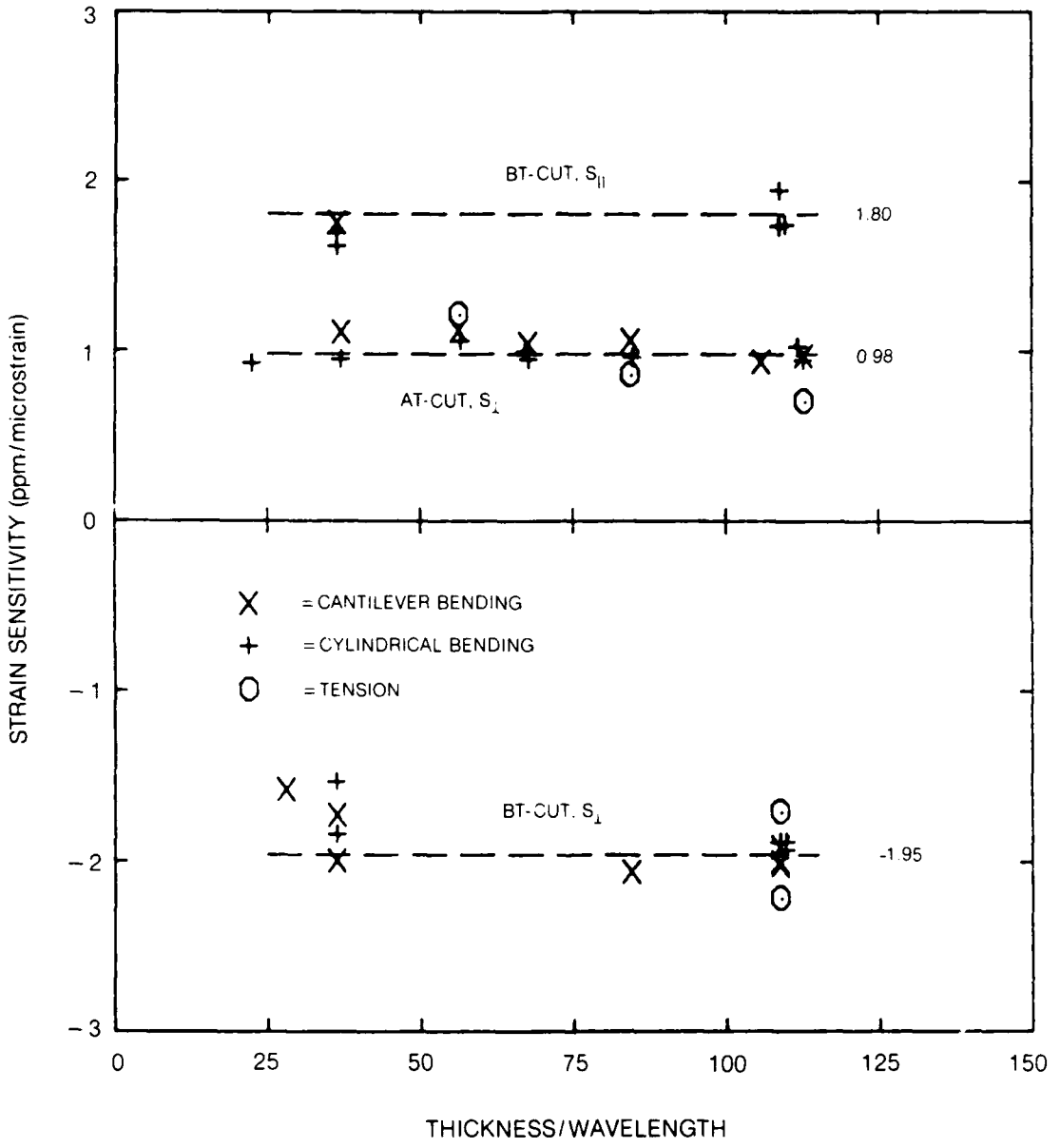

Figure 1 Strain Sensitivity Versus h/β

85-1-28-5

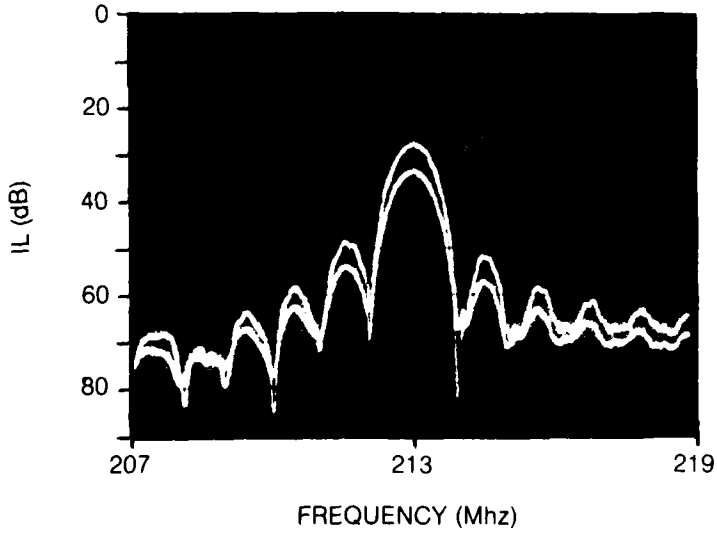

Figure 2 Effects on IL of Immerson in Oil

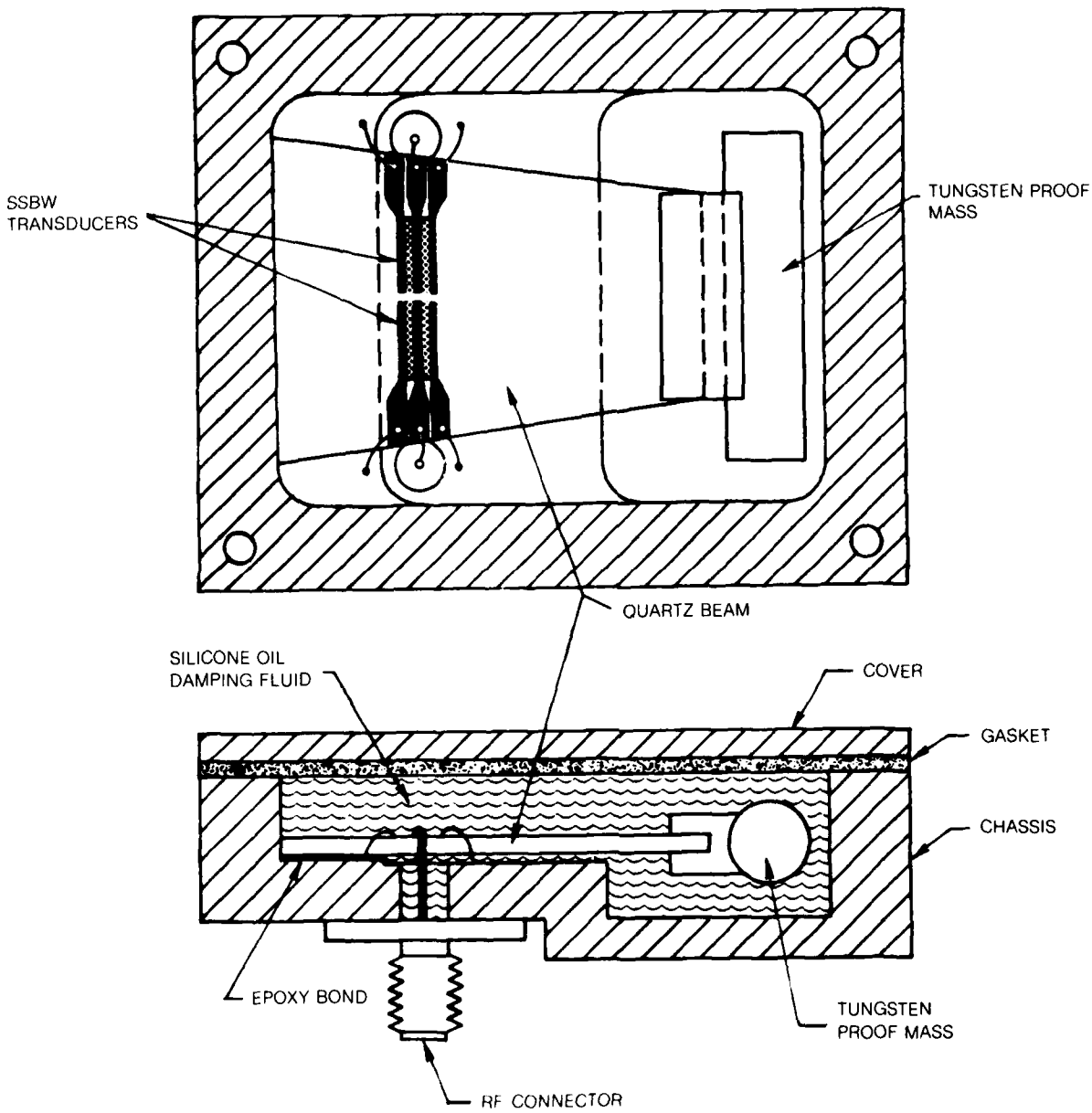

Figure 3 Laboratory Accelerometer Model

85-1-28-7

END

FILMED

5-85

DTIC